1963

Tests on welded high strength steel plate girders subjected to shear

Hai Sang Lew
Lehigh University

TESTS ON WELDED HIGH STRENGTH STEEL PLATE GIRDERS SUBJECTED TO SHEAR

by

Hai Sang Lew

A THESIS

Presented to the Graduate Faculty

of Lehigh University

in Candidacy for the Degree of

Master of Science

Lehigh University

January, 1963

CERTIFICATE OF APPROVAL

This thesis is accepted and approved in partial fulfillment of the requirements for the degree of Master of Science.

JAN 9, 1963
Date

Professor Lynn S. Beedle
Thesis Supervisor

Professor W. J. Eney, Head
Department of Civil Engineering

ACKNOWLEDGEMENTS

This thesis presents a part of an investigation made by the research project on Welded Plate Girders.

The investigation was conducted at Fritz Engineering Laboratory, Lehigh University, Bethlehem, Pennsylvania. Professor William J. Eney is Head of the Civil Engineering Department and of the Laboratory, and Dr. Lynn S. Beedle is Director of the Laboratory. The American Institute of Steel Construction, the Pennsylvania Department of Highways, the U. S. Department of Commerce-Bureau of Public Roads, and the Welding Research Council jointly sponsored the research project.

The author wishes to express his gratitude to his thesis supervisor, Dr. Lynn S. Beedle, for his guidance, and to Messrs. Bung Tseng Yen and Peter B. Cooper for helpful suggestions and constructive criticism given in the course of the thesis preparation. Sincere appreciation is also due to Dr. Konrad Basler for his valuable advice.

Special thanks are due to Mr. Kenneth P. Harpel, Laboratory Foreman, for his cooperation during the testing program, to Mr. Richard N. Sopko for preparing the drawings, and Miss Marilyn L. Courtright for typing the manuscript with great care.

TABLE OF CONTENTS

LIST OF FIGURES

1. INTRODUCTION

A research program on welded plate girders has been in progress at Lehigh University since 1957. One recent phase of this research has been the study of the shear strength of plate girders made of high strength steel.

An earlier project report presented a theoretical determination of the ultimate strength of plate girders subjected to shear.[1] In this report it was shown that the shear strength of a girder panel can be expressed as

$$V_u = V_p f(\alpha, \beta, \epsilon_y), \tag{1}$$

where V_p is the plastic shear force or the product of the web area and the yield point of the web material, α is the panel aspect ratio or ratio of panel width to depth, β is the web slenderness ratio or ratio of web depth to thickness and ϵ_y is the yield strain or ratio of yield stress to the modulus of elasticity.

To investigate the shear strength of plate girders experimentally, a series of tests were conducted.[2] In that series the aspect ratio was varied from 0.5 to 3.0 while the web slenderness ratios of the test girders varied from about 100 to about 380; however, since the girders were all made of mild steel, the yield strain parameter was essentially constant. The results of these tests showed that the theory represented by Eq. 1 (and reviewed in Section 4 of this report) can be used to predict the shear strength of mild steel girders.

The question naturally arises whether the shear strength theory is applicable for values of yield strain higher than that of mild steel. The purpose of the investigation to be presented in this report was to

answer this question. By examining girders with geometry similar to that of previously tested mild steel girders, attention was focused on the influence of yield strain. A steel with an extreme value of yield strain was selected so that if the theory proved to be adequate to describe the test girders' behavior, it could then, by interpolation, be used for girders having any value of yield strain without conducting additional tests.

Two test girders, designated H1 and H2, were fabricated from a heat treated high strength steel having a static yield level between 100 and 110 ksi. Two tests were conducted on each girder; these tests were designated T1 and T2. The values of the girder parameters for the four tests are listed in Table I.

Test	α	β	$\epsilon_y = \sigma_y/E$
H1-T1	3.0	127	0.00365
H1-T2	1.5	127	0.00365
H2-T1	1.0	128	0.00372
H2-T2	0.5	128	0.00372

Table I

Since the procedures used in determining girder dimensions and material properties and in making test measurements are similar to those used previously in tests on mild steel girders, reference should be made to the report on these tests[2] for a more detailed description.

In the following, the test specimens and test conditions will first be described, then the results will be presented. A brief review of the shear strength theory and a discussion of the correlation between test results and theoretical predictions will lead to conclusions regarding the shear strength of girders made of high strength steel.

2. DESCRIPTION OF TESTS

2.1 Girder Specimens

The two test girders had an overall length of 27'-7" and differed only in the spacing of intermediate stiffeners and the length of cover plates (Fig. 1). Webs with a depth of 50" and a thickness of 3/8" were used. Transverse stiffeners were used in pairs and were cut 3/4" short of the tension flange.(3) The bearing stiffeners were also used in pairs and were cut 3/4" short of the tension flange at the point of load application while at the ends they were cut 3/4" short of the top flange. End plates extending the full depth of the web and full width of the flanges were also used.(1) Girder H1 had partial length cover plates while girder H2 had full length cover plates. As previously mentioned, the intermediate stiffener spacing (aspect ratio) was one of the main test parameters. The partial length cover plates and the end plates provided opportunities for side studies which will be discussed in a later report.

By chosing only two plate thicknesses (3/8" and 1") for all girder components, the girders could be fabricated from a minimum number of universal plates and thus the material properties were kept as uniform as possible. Diagrams of the arrangement of the girder components on the rolled plates are shown in Figs. 2 and 3. In addition to the girder components, coupon plates were also cut from these rolled plates to be used not only to obtain tensile test coupons but also for measuring the actual girder dimensions. These measurements are summarized in Table II.

GIRDER	COMPONENT	DIMENSIONS (in)
H1	Top Cover Plate	17.03 x 0.982
	Top Flange	18.06 x 0.977
	Web	50 x 0.393
	Bottom Flange	18.06 x 0.983
	Bottom Cover Plate	17.03 x 0.982
H2	Top Cover Plate	17.06 x 1.008
	Top Flange	18.06 x 1.008
	Web	50 x 0.390
	Bottom Flange	18.06 x 1.004
	Bottom Cover Plate	17.09 x 1.008

Table II

The 8" standard tensile test coupons, which were cut from the coupon plates, were tested to determine the static yield level, ultimate tensile strength (σ_u) and percent elongation. The static yield level is defined as the yield stress obtained under a zero strain rate[2], and is referred to elsewhere in this report simply as the static yield stress σ_y. A typical load-strain curve plotted by an automatic recorder during the coupon tests is reproduced in Fig. 4. The results of the coupon tests are given in Table III.

The heat treated high strength steel used for the test girders is identified by the trade name N-A-XTRA 100. All 3/8-in. material came from one heat while all 1-in. material came from another heat. The chemical properties of these heats are listed in Table IV.

GIRDER	COMPONENT	σ_y(ksi)	σ_u(ksi)	Elong. % in 8"
H1	Top Cover Plate	105.8	117.0	14.2
	Top Flange	102.0	115.0	18.0
	Web	108.1	116.6	11.0
	Bottom Flange	110.8	121.0	14.1
	Bottom Cover Plate	105.8	117.0	14.2
H2	Top Cover Plate	108.8	120.0	15.4
	Top Flange	108.8	120.0	15.4
	Web	110.2	119.2	12.6
	Bottom Flange	102.1	114.4	15.6
	Bottom Cover Plate	108.8	120.0	15.4

Table III

Plate	C	Mn	P	S	Si	Cr	Zr	Mo
1"	0.18	0.87	0.014	0.017	0.51	0.68	0.08	0.20
3/8"	0.17	0.70	0.009	0.019	0.55	0.53	0.08	0.20

Table IV

The girders' component parts were connected by 1/4" fillet welds except around the ends of the partial length cover plates of girder H1 where 3/8" fillet welds were used (Fig. 1). The submerged arc process was employed for the welds between flanges and webs while manual welding was used elsewhere. All of the weld material had a nominal minimum tensile strength of 70 ksi.

2.2 Test Setup

The girders were tested in the simply supported condition with roller supports at the ends and essentially a concentrated load at midspan producing constant shear forces and linearly varying moments (Fig. 5). The heavy flanges to resist bending moments and the medium web thickness were selected in designing the girders so that with this test setup, failure would occur in the webs due to shear, since the primary purpose of the tests was to investigate the shear behavior of the girders. That shear failures were to be expected was verified by constructing an "interaction diagram"[4] for each test (Fig. 6). In each diagram the inclined ray from the origin represents the loading condition. Intersection of this ray with the horizontal portion of the failure envelope indicates failure due to shear. The calculation of these interaction diagrams is given in the Appendix.

Load was applied to the girder from the crosshead of the 5,000,000 lb. Baldwin Hydraulic Universal Testing Machine through a semi-spherical bearing block. The crosshead could move only in the vertical direction, thus preventing any horizontal movement of the girders at midspan. To prevent tilting of a girder, two pipes of 2 1/2" diameter braced the compression flange. These pipes were connected to the girders just below the top flange at points 75" from the end supports. The other ends of the bracing pipes were connected to a rigid, horizontal beam which was mounted on one of the machine columns. Snug fitting 1" diameter pins at each end of these pipes permitted some vertical deflection while resisting horizontal movement. In Fig. 7, a photograph showing an overall view of the test setup, the bracing arrangement can be clearly seen.

2.3 Instrumentation

During the tests measurements of vertical girder deflection were made to check the general performance of the girders while various web measurements, similar to those made on mild steel girder webs, were intended to reveal the load response of the main shear-carrying component of each girder.

Two independent systems for recording vertical girder deflection provided a constant check for each other during testing. The first consisted of an engineer's level and scales graduated to 0.01". Scales were mounted at the centerline and over the supports of each girder (Fig. 8) and on a nearby building column (as a reference scale). Level readings on a centerline scale gave the absolute deflection of the girder; relative deflection between centerline and end supports could be obtained by making corrections for support settlements. A dial gage located under a girder at the centerline constituted the second deflection measuring system. The gage stem movement, indicated to 0.001", was a convenient means of checking the deflection during loading.

It was expected that out-of-straightness of girder webs would exist before load application and that such web deflections would increase gradually with load. To measure the initial web configuration and subsequent deflected shapes, a special dial gage rig was employed[2]. The rig consisted of a portable, rigid frame on which were mounted seven dial gages for measuring movement to 0.001 in. First, the rig was placed against a machined plane surface for calibration. It was then placed against a girder web at selected sections both before a test was started and at various loads during the test. The difference between these readings and those obtained from the calibration surface gave the initial web deflections

and later deflection configurations at the seven gage locations.

Strains at a few points on a girder web were measured using rosettes of SR-4 (A1) electrical resistance strain gages (Fig. 7). Because of the deflection of a girder web, a rosette recorded a combination of membrane strain and plate bending strain rather than the former alone. By placing identical rosettes opposite each other (each side of the web), it was possible to separate these two types of strain: the average of the readings from two opposite rosettes was the strain in the middle plane of the web (membrane strain).

Elongations across the tension diagonal of a panel were measured with a hand entensometer to determine the distribution and variation of strain. While the extensometer was similar to a Whittemore gage, it had a 3 1/2" gage length and indicated changes in the gage length to 0.0001". The orientation and arragement of the extensometer gage points for test H2-T1 are shown in Fig. 9 where typical results are also indicated. Due to the fact that repetitive readings of the extensometer differed slightly, three readings were taken at each location, and the average of the three was regarded as the elongation.

Finally, to obtain a visual, qualitative indication of the location and extent of strain, all the test girders were coated with whitewash prior to testing. Under high strain, pieces of the brittle mill scale and whitewash would flake off the surface of the steel.

2.4 Testing Procedure

Testing of a girder was initiated by taking readings on all instruments at zero load (load No. 1). After that, load was applied gradually up to a predetermined level (load No. 2), where measurements were again made. This procedure was continued until inelastic behavior of the girder was observed (as indicated by a substantial increase in deflection per unit load), at which point the load was reduced to zero. This completed the first phase (cycle) of loading. Starting from zero load, the step-by-step loading procedure was again used in the second loading phase, this time all the way to ultimate load. The first test (T1) on a girder was terminated with the removal of load after ultimate load had been reached.

The attainment of ultimate load was accompanied by failure of one (or more) of the girder panels. A second test (T2) on a girder was made possible by reinforcing the panels failed in the first test such that the repaired panels would be stronger than the remaining original panels. This failure-and-repair sequence is illustrated in Fig. 10 where failure in a panel is indicated by the corresponding yield lines and the reinforcing stiffeners are drawn in dashed lines.

The second test on a girder was carried out in the same manner as the first, except that after ultimate load had been reached in the second test and thus when no additional tests were planned, an unloading curve was obtained by imposing additional deflection on the girder and recording the corresponding loads.

The use of two loading phases in each test should be further discussed. It has been established that, in tests on welded, mild steel structures, measurements taken while loading the structure for the first time can be misleading due to the presence of residual stresses.(5) During the second load cycle, however, residual stresses will have no effect for loads below the maximum load of the first cycle. With this in mind, two loading cycles were used in all tests on the high strength steel girders. As will be shown later, the influence of residual stresses during the first load cycle was not nearly as pronounced in the high strength steel girders as it is in mild steel girders.

Due to the dynamic loading effect, a definition must be formulated to specify the magnitude of an applied load in the inelastic range of girder behavior. For these tests the applied load was defined as the load corresponding to a zero strain rate, that is, the load level after load had stabilized. Thus the ultimate load was the maximum static load which a girder could sustain.

A graphical picture of the general test procedure can be obtained by referring to the load-deflection diagrams for the two girders. These diagrams, Figs. 11 and 12, will be described in the following section.

3. EXPERIMENTAL RESULTS

3.1 General Girder Behavior

The general behavior of a girder can be depicted by a load-deflection diagram. For girders H1 and H2, the applied load has been plotted against centerline deflection to form Figs. 11 and 12, respectively. In these figures, the thin solid lines labeled v_{th} represent the elastic centerline deflection curves which were calculated using beam theory including the effect of shear deformation.[2] The numbers assigned to each load for ease of reference are shown beside the plotted points. Also shown in the diagrams are the theoretical shear buckling loads (P_{cr}) and the predicted ultimate loads ($P_u{}^{th}$) for each test. (P_{cr} and $P_u{}^{th}$ will be further defined and discussed in Section 4.)

With the load-deflection diagrams available, the complete testing history of each girder can be traced, including the two tests on a girder, the two cycles of loading and the stabilizing of loads in the inelastic region. It can be seen from Figs. 11 and 12 that, unlike mild steel girders, the load-deflection behavior of the high strength steel girders did not change significantly in the second load cycle. This is an indication that residual stresses do not play as great a role in high strength steel girders. It is also clear from the diagrams that in each test the strength of a girder differed considerably from the web buckling load, and that beyond the maximum load a girder lost its strength only gradually as increasing deflections were imposed on it (tests H1-T2).

With reference to Figs. 11 and 12, girder behavior for each individual test will now be reviewed.

Test H1 T1

Girder H1 initially had one long panel with $\alpha = 3.0$ and two shorter panels with $\alpha = 1.5$. Failure was expected to occur in the long panel in test H1-T1. As was anticipated, no sudden buckling of the web occurred at its theoretical buckling load of 377 kips; the web merely deflected gradually in the lateral (z) direction with increasing load. The first flaking of white-wash was observed on the web at around 600 kips. When the applied load reached about 670 kips (between load Nos. 5 and 6), a sudden rumbling was heard. The web was found to have "snapped-through" from one deflected position to another (from the positive z side to the negative z side) while the load had remained stable. Only additional flaking of whitewash and increasingly visible web deflections were observed between this load and 900 kips, the highest of the first loading phase. The whitewash flaking clearly followed the general direction of the panel's tension diagonal.

No sudden movement of the web could be detected visually during the unloading of the first load cycle and subsequent reloading in the second load cycle, although a low rumbling was heard in the latter step. Later examination of the web deflection measurements (Section 3.2), however, showed that the web had returned to its original configuration during unloading and again snapped through when reloaded. The significance of this repeated snap-through phenomenon is that it did not cause girder failure and didn't even result in a marked temporary discontinunity of load

Above 1200 kips (load No. 18), fine yield lines started to appear on the web near the areas where whitewash flaking had previously occurred. The number of these yield lines increased with magnitude of load. Fig.

13 gives an overall view of the panel at the ultimate load, 1260 kips. Unloading of the girder completed the first test, H1-T1.

Test H1-T2

After the repair of the failed panel of test H1-T1 (Fig. 10), the girder had three panels with α = 1.0 and two with α = 1.5 where failure was expected to occur in test H1-T2. The end of the girder having the repaired panels was covered with a fresh coat of whitewash prior to starting this test. At a load of 750 kips (load No. 26), flaking of this new whitewash was observed in the repaired panels having α = 1.0. This was due to the permanent web deformations which resulted from test H1-T1: the web deflection increased faster in these already deflected panels than in those with α = 1.5. As higher loads were applied, flaking started in the longer panels while it gradually stopped in the shorter ones. At 1350 kips (load No. 29), strips without whitewash could easily be seen oriented in the general direction of the tension diagonals of the α = 1.5 panels. Load was then reduced to zero (load No. 30), completing the first loading phase.

The second loading phase of test H1-T2 produced an increasing amount of whitewash flaking as load was increased beyond 1350 kips (load No. 36). An ultimate load of 1538 kips was attained. While obtaining an unloading curve as described in Section 2.4, excessive web deflections caused slight flange tilting. Some end post bending and yielding also occurred. The yield lines in the end post may be seen at the left side of Fig. 14, a photograph taken after the test was completed and the girder removed from the testing machine. As can also be seen from the extent of yielding in the two panels, failure occurred in the panel near the girder end. The

web deflections in the inner panel were largely recovered during unloading.

Test H2-T1

Similar to girder H1, girder H2 also had two different panel sizes. Three identical longer panels with an aspect ratio of α = 1.0 were expected to fail in the first test. As in the previously described tests, no "buckling" of the web could be detected at the theoretical buckling load and flaking of whitewash occurred more and more with higher loads. The three square panels, subjected to the same shear force, performed similarly. At 1500 kips (load No. 7), the peak load of the first load cycle, it was difficult to judge visually which panel would fail first.

As the applied loading exceeded the maximum load of the first cycle (1500 kips) during the second load cycle, it gradually became apparent from the size of the yielded zones that failure would occur in the innermost of the three panels. The appearance of these panels at the ultimate load of 1834 kips is shown in Fig. 15. The test was terminated without obtaining an unloading curve since another test on the girder was planned.

Test H2-T2

Each of the three panels having α = 1.0 were repaired with the addition of two pairs of vertical stiffeners (Fig. 10) before test H2-T2 was started. Failure in this test was expected to occur in one of the six original panels having α = 0.5. The behavior of the girder during the first loading phase was about the same as that during test H2-T1. Whitewash flaking started in the six panels between 1800 and 1950 kips (load Nos. 25 and 26), and continued through the rest of the first cycle.

During the second cycle, yielding in the centermost panel became more and more pronounced as the ultimate load of 2250 kips (load No. 40) was approached. Fig. 16, a photograph taken after failure, shows the extent of yielding and shear deformation in this panel. This shear deformation increased while obtaining the unloading curve until, at load No. 43, due to the very severe bending of the compression flange, a crack about 10" long was opened in the fillet weld between the top flange and cover plate over the failed panel.

Summary of Ultimate Loads

With the exception of some minor differences, the two girders performed in a similar manner during the four tests. The experimentally obtained ultimate loads (P_u^{ex}) differed from test to test. For convenience of comparison and later discussion these loads are listed in Table V with the aspect ratios, the theoretical web buckling loads and the calculated theoretical ultimate loads (P_u^{th}) for each test. The latter two values will be more completely defined in Section 4. For further comparison the ratio of P_u^{ex} to P_u^{th} is given in the last column of the table.

Test	α	P_{cr} (k)	P_u^{th} (k)	P_u^{ex} (k)	P_u^{ex}/P_u^{th}
H1-T1	3.0	376.8	946	1260	1.33
H1-T2	1.5	464.0	1420	1538	1.08
H2-T1	1.0	594.4	1750	1834	1.05
H2-T2	0.5	1613.8	2286	2250	0.98

Table V

A part of table V is presented graphically in Fig. 17. In this figure P_u^{th} is the ordinate while the yield strain is the abscissa. A second abscissa scale is shown for the more familiar quantity of yield

stress. For a constant web slenderness ratio ($\beta = 127$), each curve represents the shear theory (see Section 4) for a given value of α. Solid dots are used to represent the test results for the high strength steel girders and for two tests on a mild steel girder (Girder E1, Ref. 2) which had a web slenderness ratio near 127. The correlation of test results with theory will be discussed later.

3.2 Web Behavior

As stated in Section 2.2, failure in each girder test was anticipated in the web due to shear. It is evident from the preceeding description of general girder behavior that web yielding and deformation caused failure in each test, as expected. In this section the various measurements taken to record the response of the web to applied load will be summarized.

Web Deflection

Initial deformations existed in the webs of both test girders; as load was applied during testing, these deformations gradually increased in magnitude. Deflected web configurations were measured using the dial gage rig described in Section 2.3. As an example, the measured configurations for one transverse section (x=+117.5) of test H1-T2 are shown in the top part of Fig. 18. The deflection data has been plotted in this figure at the seven gage points and the approximate deflection shapes shown by connecting the plotted points with straight lines. As a further indication of the gradual growth of deflections, the lateral movement of the web at middepth at the same section has been plotted against the applied load in the lower portion of the figure. At the ultimate load of 1538 kips (load No. 38), the maximum deflection w of the web was about 1 5/8 inches in the negative z - direction.

Diagrams similar to that in the upper portion of Fig. 18 have been superimposed on elevation views of the girders in Figs. 19 and 20. For each of the two tests on girder H1 (Fig. 19), deflected configurations at three sections in a panel are shown. For girder H2 (Fig. 20), the deflection patterns are shown only for the center sections of the panels.

In each case the deflected shape labeled with the lowest load number corresponds to measurements taken after the first load cycle of a test was completed and load reduced to zero. These shapes differed very little from those measured before a test was started. The magnitude of applied load corresponding to the load numbers may be found by referring to the appropriate load-deflection curve (Fig. 11 or 12). From girder H1, especially test H2, it is quite clear that the deformations formed valleys in the web which were parallel to the general direction of the tension diagonals of the panels and thus were indicative of tension field action.

Strains in Girder Webs

That the web strains conformed with deflections can be interpreted from the elongation measurements on the web. Typical hand extensometer results are shown in Fig. 9 for the end panel of test H2-T1. The location of the gage points are indicated in the lower portion of the figure and the measured strains are plotted from the centerline of the gage lengths in the upper portion. For comparison purposes, the yield strain is shown by a light solid line on the plots and is also indicated on the strain scale. It can be seen from the figure that strains increased with load and that as web deflections increased, elongations became less uniform across a set of gage lines. Approximately along the diagonal where web deflection valleys formed, the elongations were more pronounced--another indication of tension field action.

The gradual change of web strain with load can also be seen from the results obtained from SR-4 gage rosettes. Fig. 21 indicates this gradual change at two points in the end panel of test H2-T1. Principal stresses

determined from the rosette data are shown for three different loads in the figure. At a relatively low load, these principal stresses (solid lines) were about the same as those predicted using beam theory (dashed lines). When higher loads were applied, the magnitude of the measured principal stresses increased gradually in the direction of the tension diagonals. This rearrangement of stress in response to increasing load is still another indication of tension field action.

4. REVIEW OF SHEAR STRENGTH THEORY

Before comparing the test results with the theoretically predicted strength of the girders, it will be helpful to review the shear strength theory upon which these predictions are based. This theory is derived and discussed in Ref. 1 and will only be summarized briefly here.

It has long been recognized that the attainment of the web buckling stress does not limit the strength of a girder. Post-buckling strength must be evaluated to establish the carrying capacity. In the case of a girder subjected to shear, the source of post-buckling strength lies in the framing elements of the web. Anchored by the transverse stiffeners, flanges and neighboring panels, the web is able to sustain shear forces in excess of the "buckling" shear force in a manner analogous to a Pratt truss panel where the tension diagonals are supported by the vertical compression struts and the chord members.

In the development of the shear strength theory, the classical method of resisting shear by shearing stresses in the web may be termed "beam action" while the method of resisting shear by tensile membrane stresses in the web is called "tension field action". It is assumed that applied shear is carried by beam action up to the buckling load but that thereafter all additional shear is carried by tension field action. Thus the ultimate shear force is expressed as

$$V_u = V_\tau + V_\sigma, \tag{2}$$

where V_τ is the beam action contribution and V_σ is the contribution due to tension field action.

The beam action shear V_τ can be represented by the product of the web area and the critical shear stress τ_{cr},

$$V_\tau = bt\tau_{cr}, \tag{3}$$

while V_σ can be evaluated from the geometry and equilibrium of the tension field, resulting in

$$V_\sigma = \sigma_t bt/(2\sqrt{1+\alpha^2}), \tag{4}$$

where σ_t is the tension field stress and α is the aspect ratio or ratio of panel width to depth.

When the two contributions to the shear strength given by Eqs. 3 and 4 are substituted into Eq. 2, and the definitions $V_p = bt\tau_y$ and $\tau_y = \sigma_y/\sqrt{3}$ are used with some approximations, the desired shear strength formula is obtained,

$$V_u = V_p \left[\frac{\tau_{cr}}{\tau_y} + \frac{3}{2} \frac{1 - \tau_{cr}/\tau_y}{\sqrt{1 + \alpha^2}} \right] \tag{5}$$

This is the expression which was represented by Eq. 1 in the Introduction.

The buckling stress is given by

$$\tau_{cr} = k \frac{\pi^2 E}{12(1-\nu^2)} \left[\frac{t}{b} \right]^2 \tag{6}$$

where k is the shear buckling coefficient for simply-supported rectangular plates,

$$\text{or} \quad \begin{aligned} k &= 4.00 + \frac{5.34}{\alpha^2}, \text{ when } \alpha \leq 1 \\ k &= 5.34 + \frac{4.00}{\alpha^2}, \text{ when } \alpha \leq 1 \end{aligned} \tag{7}$$

For cases where τ_{cr} is above the proportional limit, a consideration of inelastic buckling or strain hardening has to be made. This topic is discussed in Ref. 1. Since τ_{cr} for each of the four tests described in this report was below the proportional limit, Eqs. 6 and 7 are applicable.

For a constant web slenderness ratio ($\beta = b/t$) and a given aspect ratio (α), the shear buckling stress is a constant which can be obtained from Eqs. 6 and 7. Consequently, the shear strength of a girder panel is a function

of τ_y alone (Eq. 5). For the setup of the test girders, $V_u = 1/2\ P_u^{th}$ (while $V_{cr} = 1/2\ P_{cr} = 1/2\ \tau_{cr}\ A_w$) and, since $\tau_y = \frac{\sigma_y}{\sqrt{3}} = \frac{E}{\sqrt{3}}\ \epsilon_y$, the theoretically predicted load P_u^{th} is a function of the yield strain ϵ_y through Eq. 5. The relationship is a linear one and is presented graphically in Fig. 17 for various values of α.

5. CORRELATION OF EXPERIMENTAL RESULTS WITH THEORY

5.1 Comparison of Observed and Predicted Strengths

The theory reviewed in the preceding section furnishes a means of predicting shear strength of a girder providing adequate anchorage for the web exists so that tension field action can develop. The deformations and strain distribution associated with the ultimate shear force are not specified by the theory. Since the two high strength steel test girders exhibited deformations and strain distributions similar to those encountered in mild steel girders[2], discussion of the test results will be concentrated on the correlation between the predicted and the actually observed ultimate loads.

In Table V the theoretical shear strength and the experimental ultimate load for each girder test are listed. From the last column of the table, it can be seen that differences between these two loads are within ten percent except in the case of test H1-T1. A difference of up to ten percent is acceptable because of the usual scattering of experimental results. (About the same deviation was obtained for the mild steel girder tests, Ref. 1.) However, the amount by which the observed ultimate load of test H1-T1 exceeded the predicted strength may not be attributed to the usual scatter.

An examination of Table V reveals that the test results exceeded the predictions to a greater extent as the aspect ratio increased. This trend is also indicated by an ultimate load vs. aspect ratio (P_u vs. α) diagram, Fig. 22. In the diagram the test results are shown with vertical bars at their respective α-values while the predicted strength is represented by a curve based on Eq. 5. If a similar diagram were plotted for the mild steel girder tests, the same trend would be observed. (See Table 1 of Ref. 1).

The difference between P_u^{ex} and P_u^{th} is less in the case of mild steel, being + 11% for test E1-T1 (Ref. 1) as compared with + 33% for test H1-T1, both with $\alpha = 3.0$. Nevertheless, the fact that this difference increases with α seems to be well established. The reason for this behavior should now be examined.

5.2 Influence of Panel Boundaries

It was pointed out in Section 4 that the shear strength of a girder is assumed to consist of two parts: "beam action" and "tension field action". In the formulation of the theory, it was suggested that the beam action contribution should be computed using a simply-supported (hinged) edge condition for the web panels (Eq. 7). If the actual boundary conditions are such that the web is partially restrained along the flanges, what is the effect of aspect ratio on the beam action contribution?

Since the influence of boundary conditions is reflected in the shear buckling coefficient k, the variation of the beam action contribution with α can be explained with the aid of a k vs. α diagram. Such a diagram is shown in Fig. 23 for two extreme cases. the most flexible condition of simply-supported edges all around and the condition of full restraint along the flanges and simply-supported along the stiffeners.[6] For both cases, the beam action contribution changes with aspect ratio. The difference in k-values amounts to about 5% for α = 0.5 and about 66% for α = 3.0. This means that for small values of α (narrow panels), the actual beam action contribution can differ only slightly from the computed value, while for higher values of α (long panels) the boundary restraint may increase the beam action contribution to a greater extent.

The effect of boundary conditions on the total shear strength, however, differs from that on beam action. The latter is only one of the two contributions to the shear strength (Eq. 2). Because the tension field action part is related to the beam action part through a yield condition[1], a larger amount of beam action leaves a smaller margin for the development of tension field action. The net result is that for long panels (high α),

boundary restraint increases shear strength above the value predicted using simply-supported edges, but this effect is not as pronounced as it is for beam action alone.

The actual shear strength increase does not only depend on the aspect ratio α and the boundary conditions which have been discussed above. It is also affected by the web slenderness ratio β, the yield stress and the residual stresses in a girder. Providing all other parameters are held constant, a relatively low value of β (stocky web) results in beam action contributing a large proportion of the shear strength. In this case the possibility of the ultimate shear load to exceed the prediction is relatively high (at least for long panels). For higher β - values (slender webs), beam action contributes only a small amount while tension field action predominates; thus the influence of edge restraint is likely to be smaller.

5.3 Effect of Residual Stresses

The reasoning of Section 5.2 accounts for the deviation between the test results and predictions for long panels. It does not explain why this deviation is greater for high strength steel girders. The answer to this question lies mainly in the existance of residual stresses in plate girders, especially welded plate girders.

The residual stresses at the web-to-flange fillet welds are tensile stresses of high intensity, equal in magnitude to the yield point of the weld material.(7) For mild steel girders this yield point is in general higher than that of the base metal. Along the heat affected zone adjacent to the welds, the magnitude of the residual stress is often comparable to the yield point of mild steel. Adding to this the bending and shear stresses which arise in developing the strength of a girder, a strip of yielded material is often formed along the flanges, resulting in a yield hinge. Thus the restraint on the web is reduced and the situation is closer to the simply-supported boundary condition. Accordingly, such a condition is assumed in the formulation of the shear strength theory.

For high strength steel girders, such as those described in this report, the yield point of the base metal is higher than that of the metal (about 110 ksi to 70 ksi for the present case). There exists a large margin between the yield point and the residual stress along the welds and thus the chance of forming a yield hinge is reduced. For these girders, then, the boundary condition for the web along the flanges is closer to clamped than simply-supported. As longer panels are used, the beam action contribution exceeds that for mild steel girders more because of this restraint, and the observed shear strength becomes higher than the prediction accordingly.

It would seem logical to assume in the theory that, for high strength steel girders, the web is partially restrained by the flanges. However, a difficulty arises in the determination of the amount of restraint which actually develops. This is not only a function of the girder geometry but also is affected by the magnitude of the residual stresses as explained above. Until more quantitative information is available on the latter, it would be safe to assume simply-supported edges along the flanges for girders made of any steel.

6. CONCLUSIONS

The shear strength theory developed in Ref. 1 predicts that, for plate girders having the same geometry, shear strength is related to the yield stress of the girder material as shown in Fig. 17. This prediction has now been confirmed by the tests described in this report.

If any trend can be seen from the four tests, it is that the tendency for the theory to be conservative for girders with long panels may be more pronounced when the girders are made of high strength steel.

Since the theory is applicable for mild steel girders and for high strength steel girders, by interpolation it must also be applicable for girders made of other steels with yield points between these two extreme cases. Therefore, it is recommended that this shear strength theory be used for all presently available structural steels.

NOMENCLATURE

A_w = web area, bt

E = modulus of elasticity, 29,600 ksi.

M = applied bending moment

M_u = ultimate bending moment

M_y = yield moment

P = applied jack load, 2V

P_{cr} = theoretical shear buckling load, $\tau_{cr} A_w$

P_u^{ex} = experimentally observed ultimate load

P_u^{th} = theoretical ultimate load, $2V_u$

V = applied shear force

V_p = plastic shear force, $\tau_y A_w$

V_u = theoretical ultimate shear force

V_σ = tension field action shear force

V_τ = beam action shear force

b = web depth

k = shear buckling coefficient

t = web thickness

v_ℓ = vertical deflection at girder midspan

w = web deflection (in z direction)

x,y,z = Cartesian coordinates (in inches) having origin at geometric center of the girder web

α = aspect ratio, ratio of panel length to web depth

β = slenderness ratio, ratio of web depth to web thickness

ϵ = strain

ϵ_y = yield strain, σ_y/E

ν = Poisson's ratio, 0.3

σ_t = tension field stress

σ_u = ultimate tensile stress

σ_y = yield stress

τ_{cr} = theoretical shear buckling stress

τ_y = shear yield stress, $\sigma_y/\sqrt{3}$

APPENDIX

Use of Interaction Diagram to Predict Failure Mode

The results of a study[4] of possible interaction between moment and shear are shown below in an interaction diagram. In the diagram the ordinate is the ratio of the applied shear force V to the ultimate shear force V_u and the abscissa is the ratio of the applied bending moment M to the yield moment M_y, where M_y is defined as the moment required to initiate yielding at the extreme fiber of the compression flange. When the geometry and material of a girder are specified, the diagram can easily be constructed.

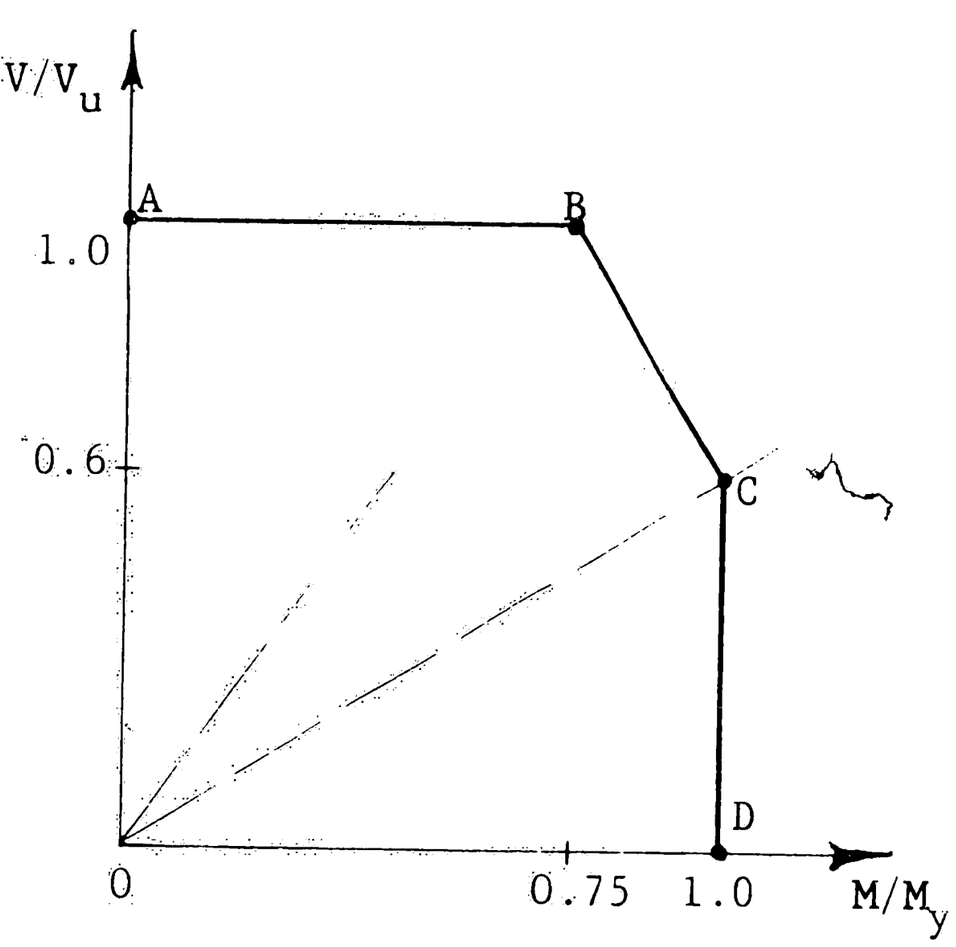

The interaction diagram is useful for predicting the mode of failure to be expected of a girder subjected to a given loading condition. If a ray is plotted passing through the origin and having a slope representing the given loading condition, the interaction of this ray with the diagram specifies the failure mode to be expected. An intersection with the horizontal part AB indicates a shear failure, one with the vertical line CD indicates a bending failure and one with the inclined portion BC predicts a failure due to the combined effects of moment and shear.

As an example, calculations will be shown for test H1-T1. From the dimensions of the girder and yield point of the steel, the yield moment and the ultimate shear force were computed:

$$M_y = 194{,}000 \text{ kip-in.}$$

$$V_u = 473 \text{ kips}$$

The slope of the ray representing the test conditions can be expressed as

$$\frac{V}{V_u} \div \frac{M}{M_y} = \frac{P/2}{V_u} \div \frac{Px/2}{M_y} = \frac{M_y}{V_u x},$$

where x is the moment arm to the critical section.[8] Numerically, using a value of x = 125",

$$\text{Slope} = \frac{194{,}000}{473 \times 125} = 3.28$$

The resulting interaction diagram is shown in Fig. 6 along with those for the other tests. It is seen from the diagrams that a shear failure is indicated for all four tests.

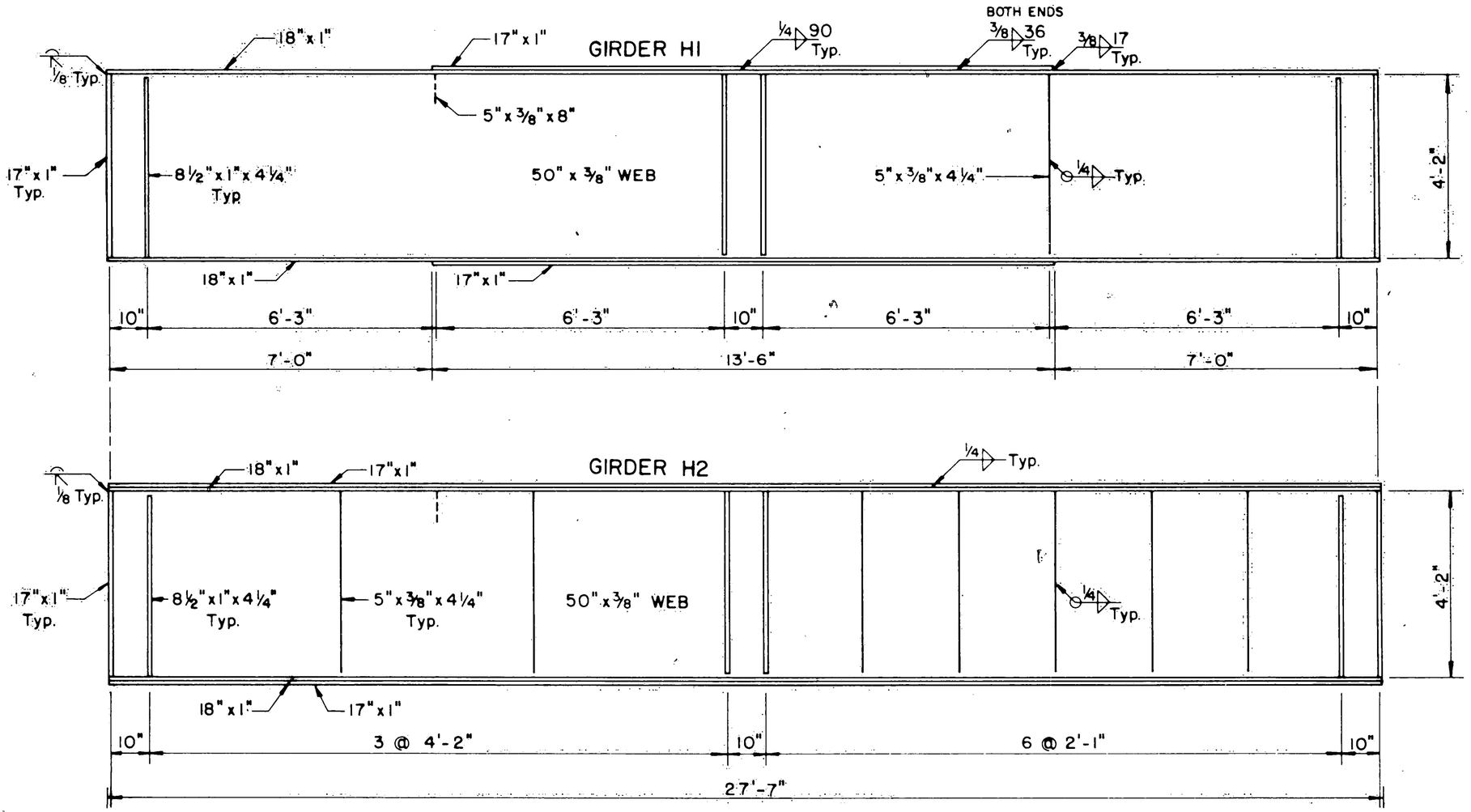

Fig. 1 Test Girders H1 and H2

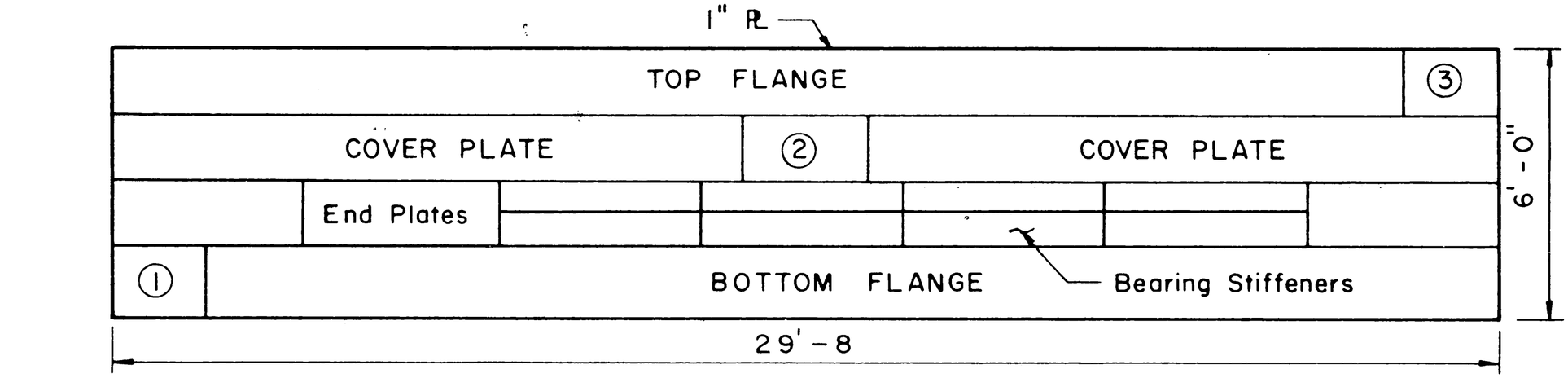

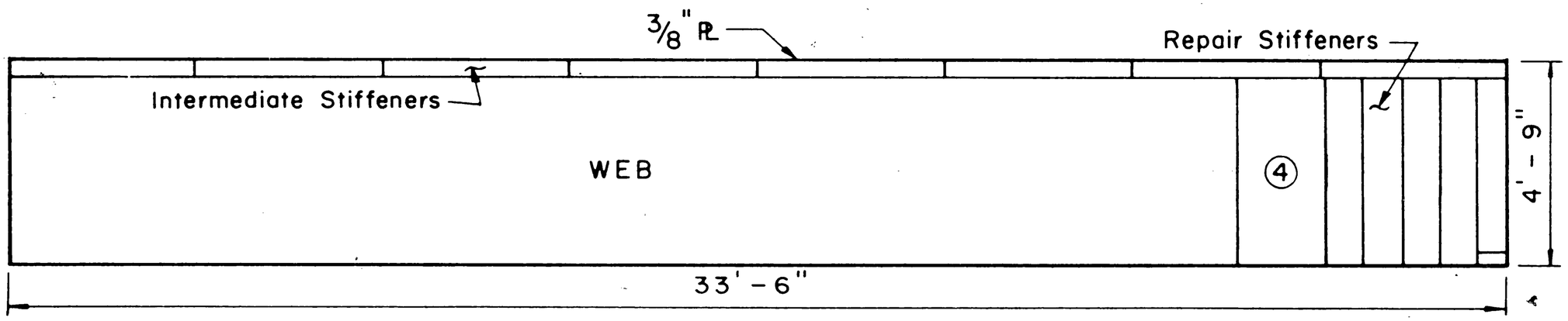

① Denotes Coupon Plate

Fig. 2 Cutting Diagram for Girder H1

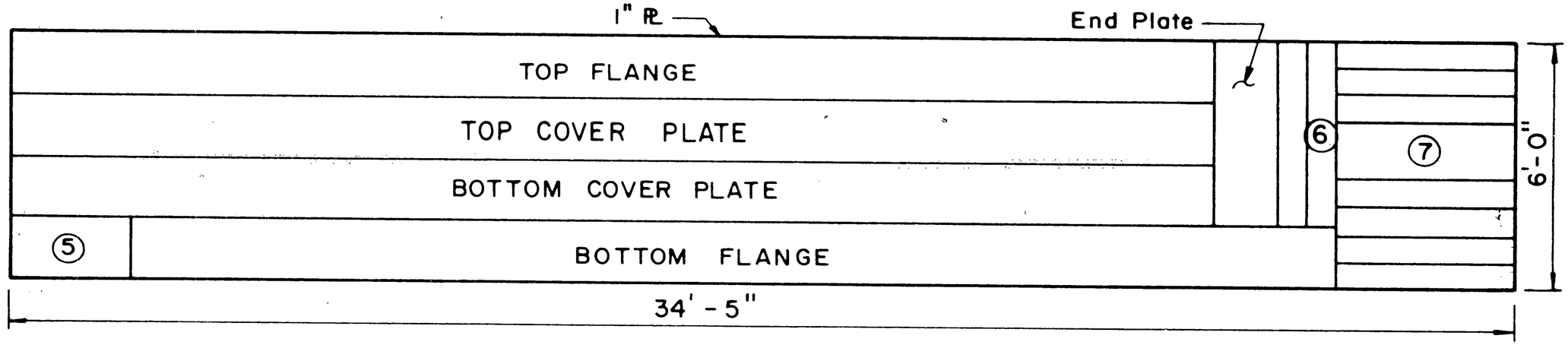

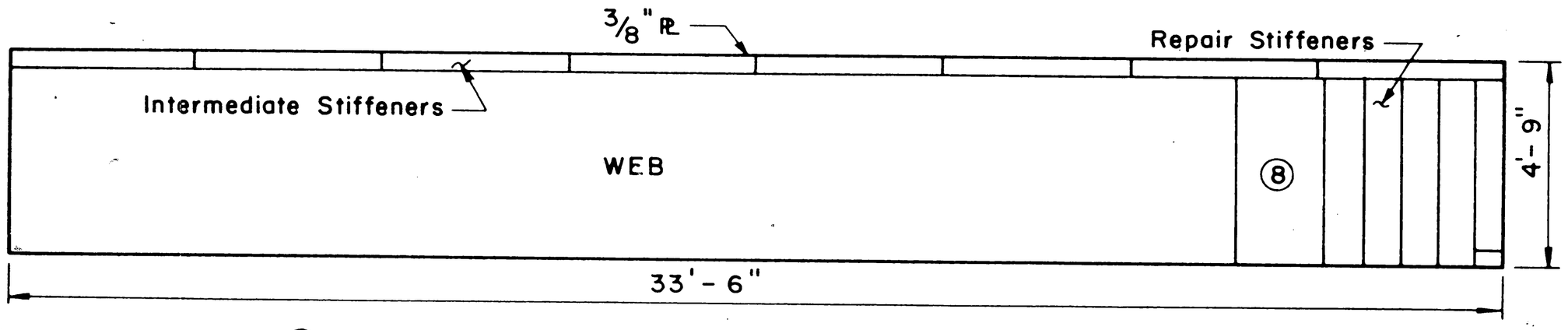

⑤ Denotes Coupon Plate

Fig. 3 Cutting Diagram for Girder H2

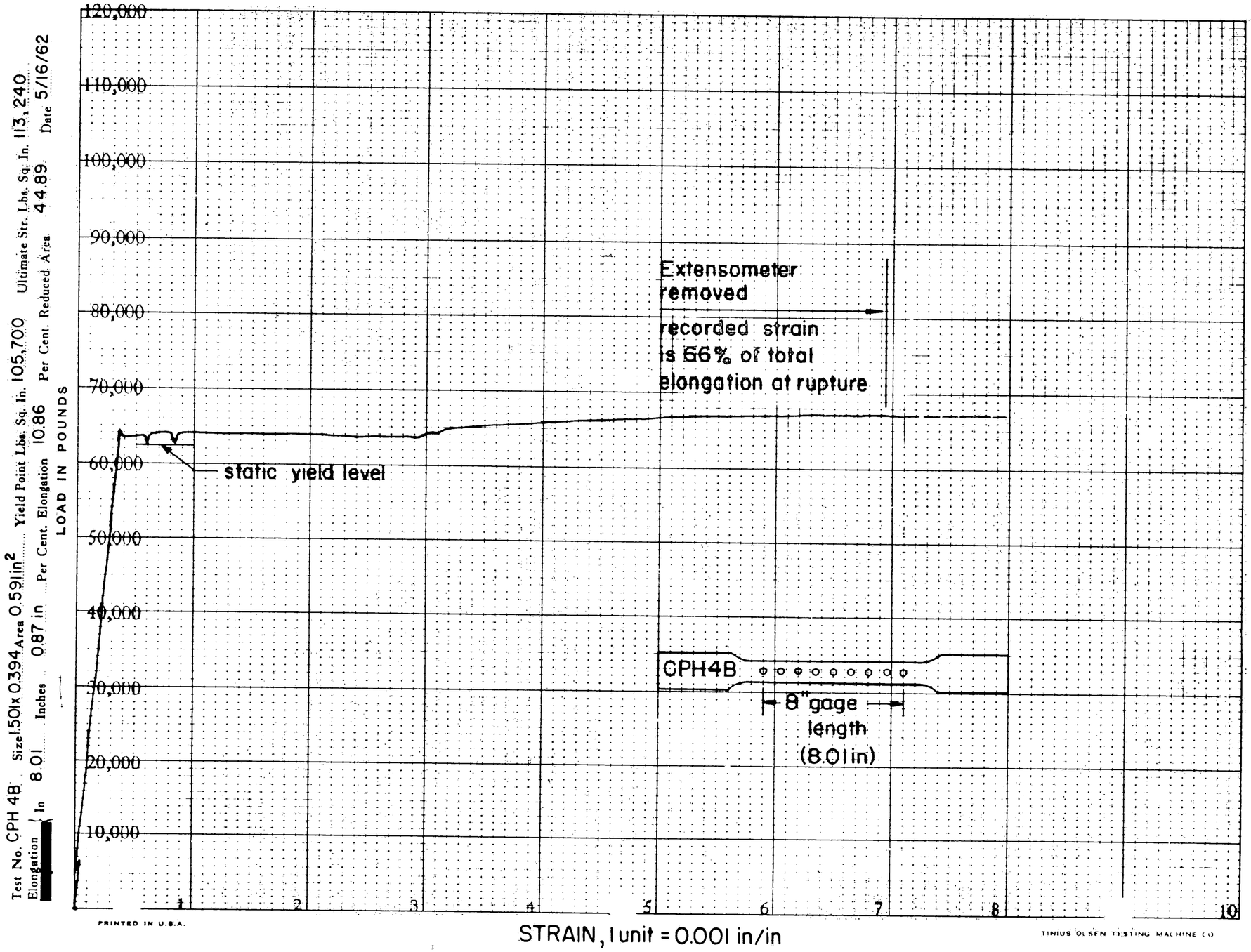

Fig. 4 Typical Coupon Test Results

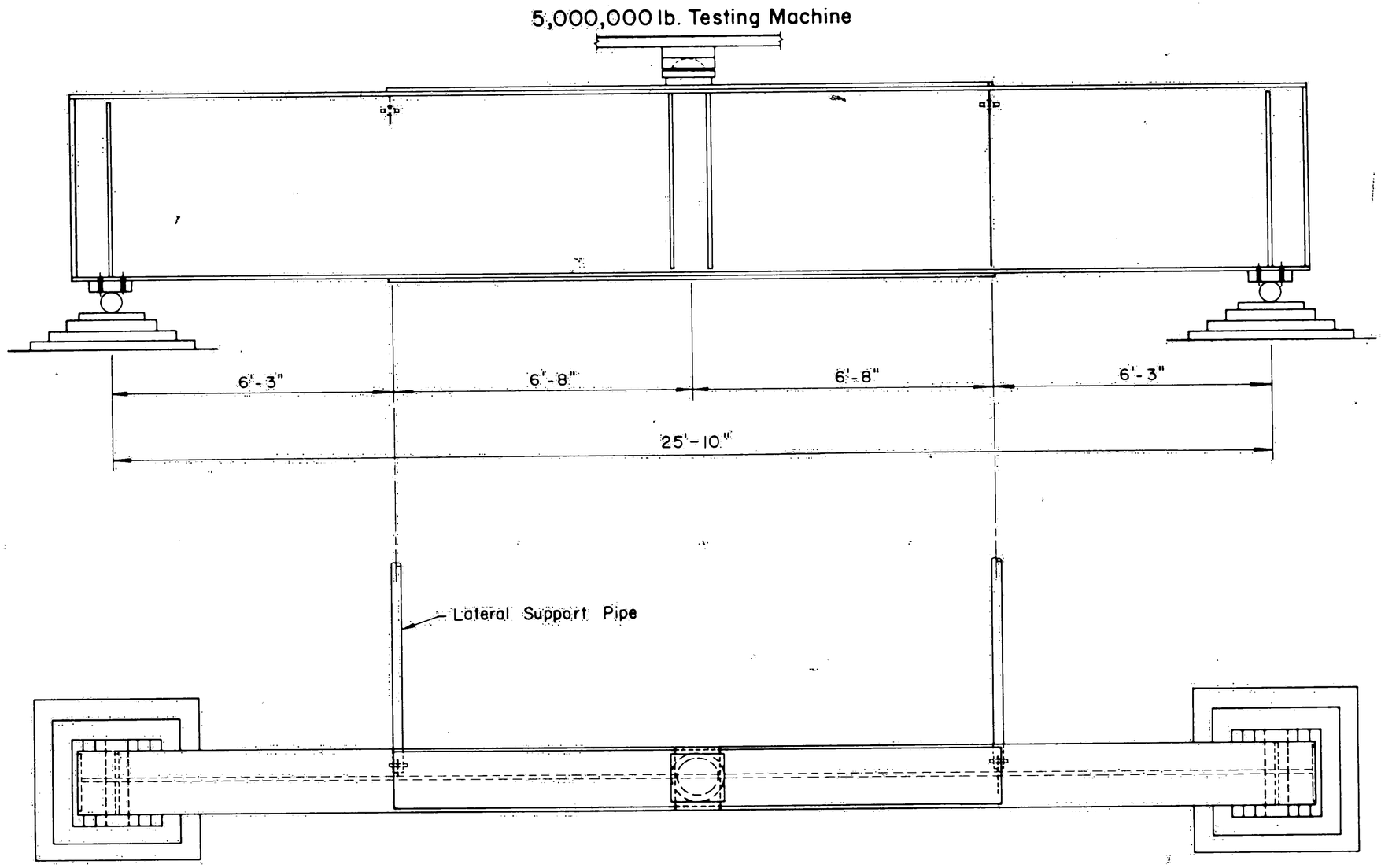

Fig. 5 Test Setup

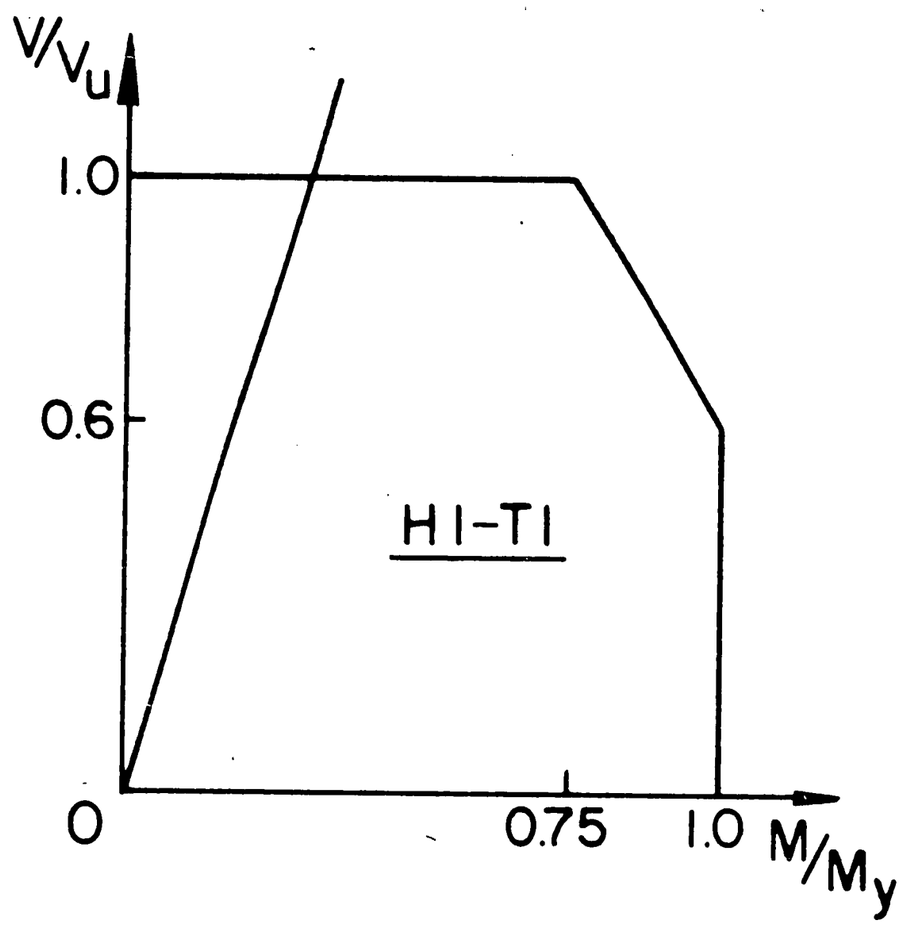

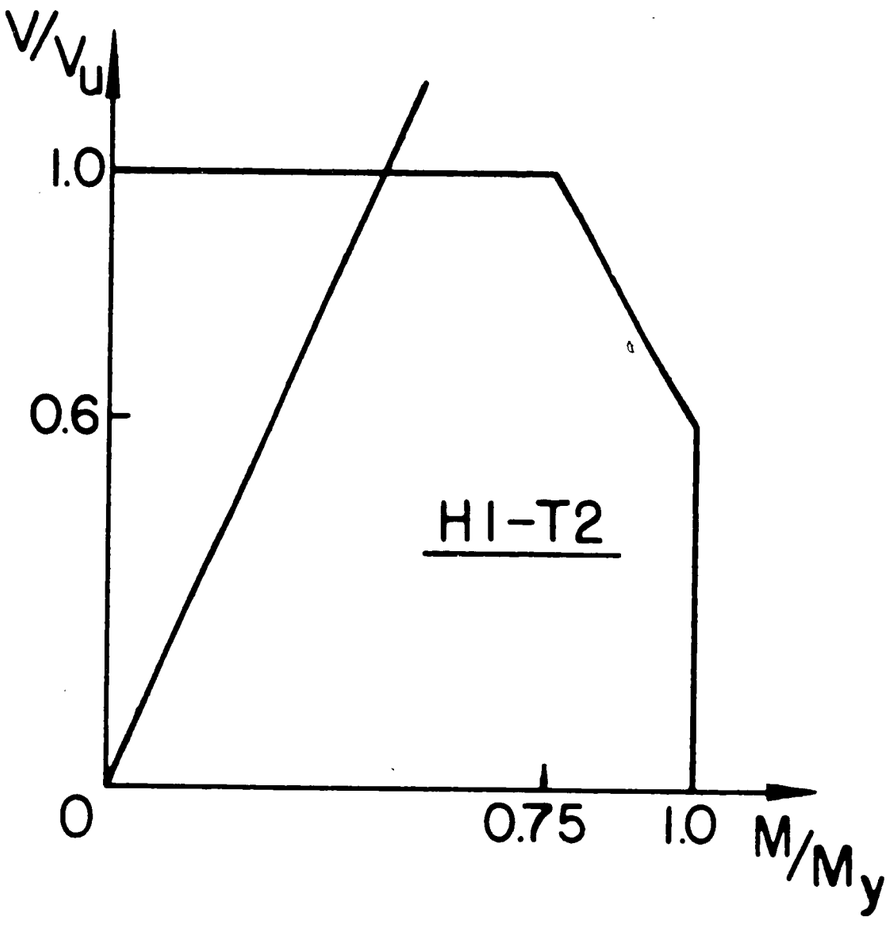

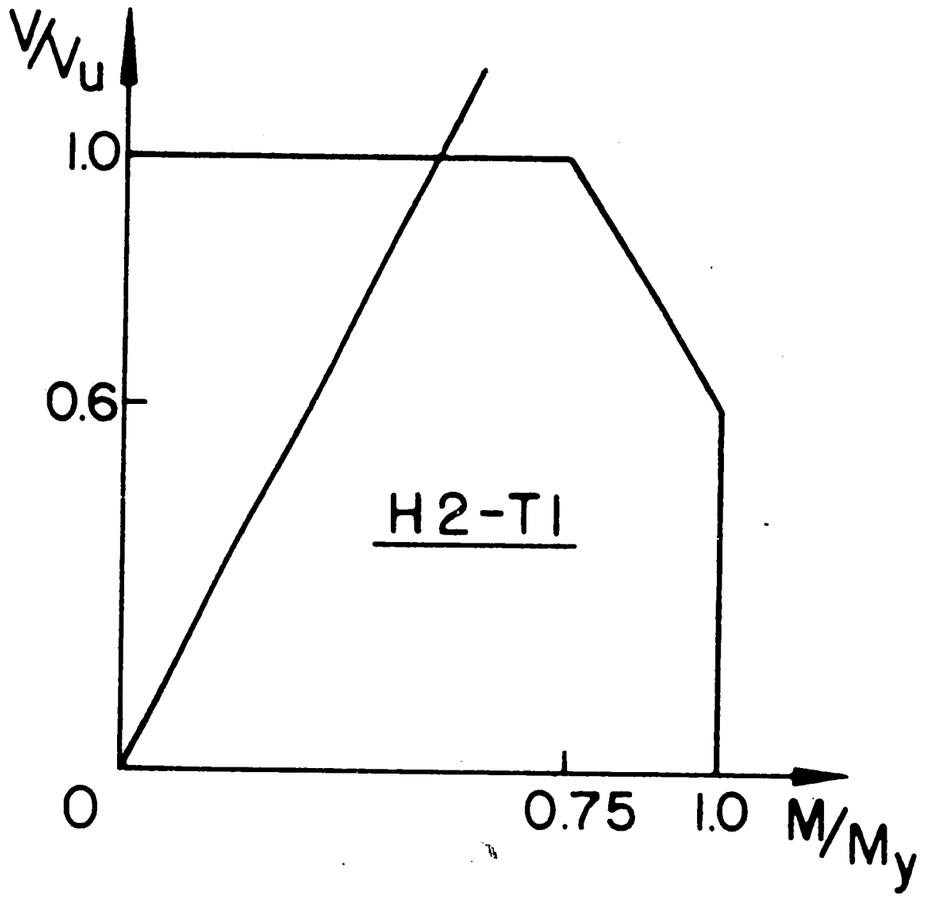

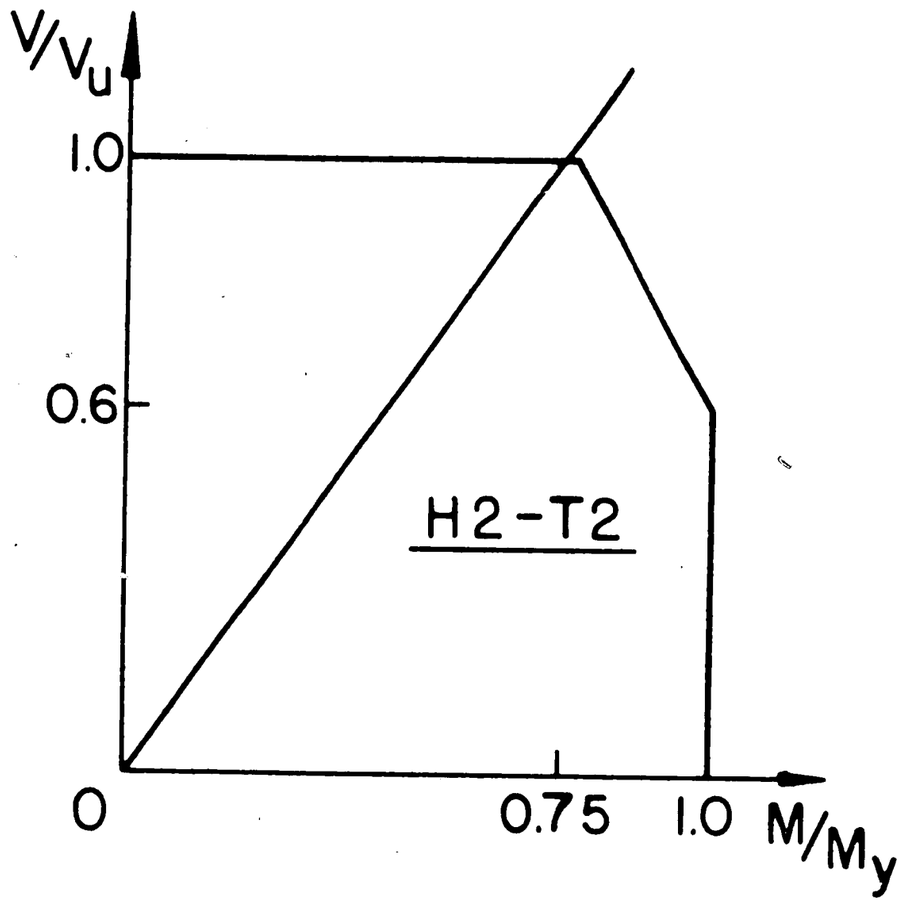

Fig 6 Interaction Diagrams

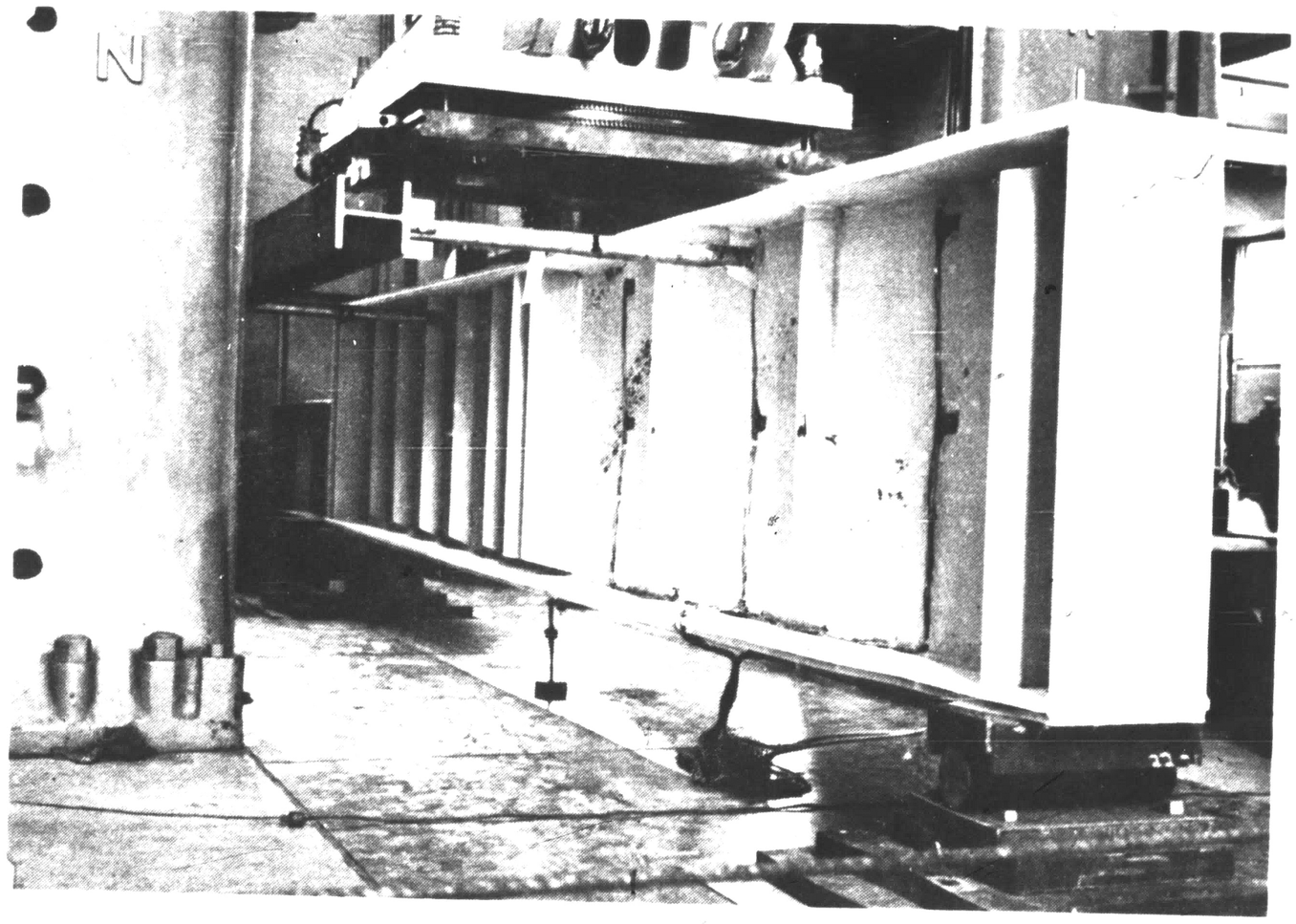

Fig. 7 Test Setup (Girder H2)

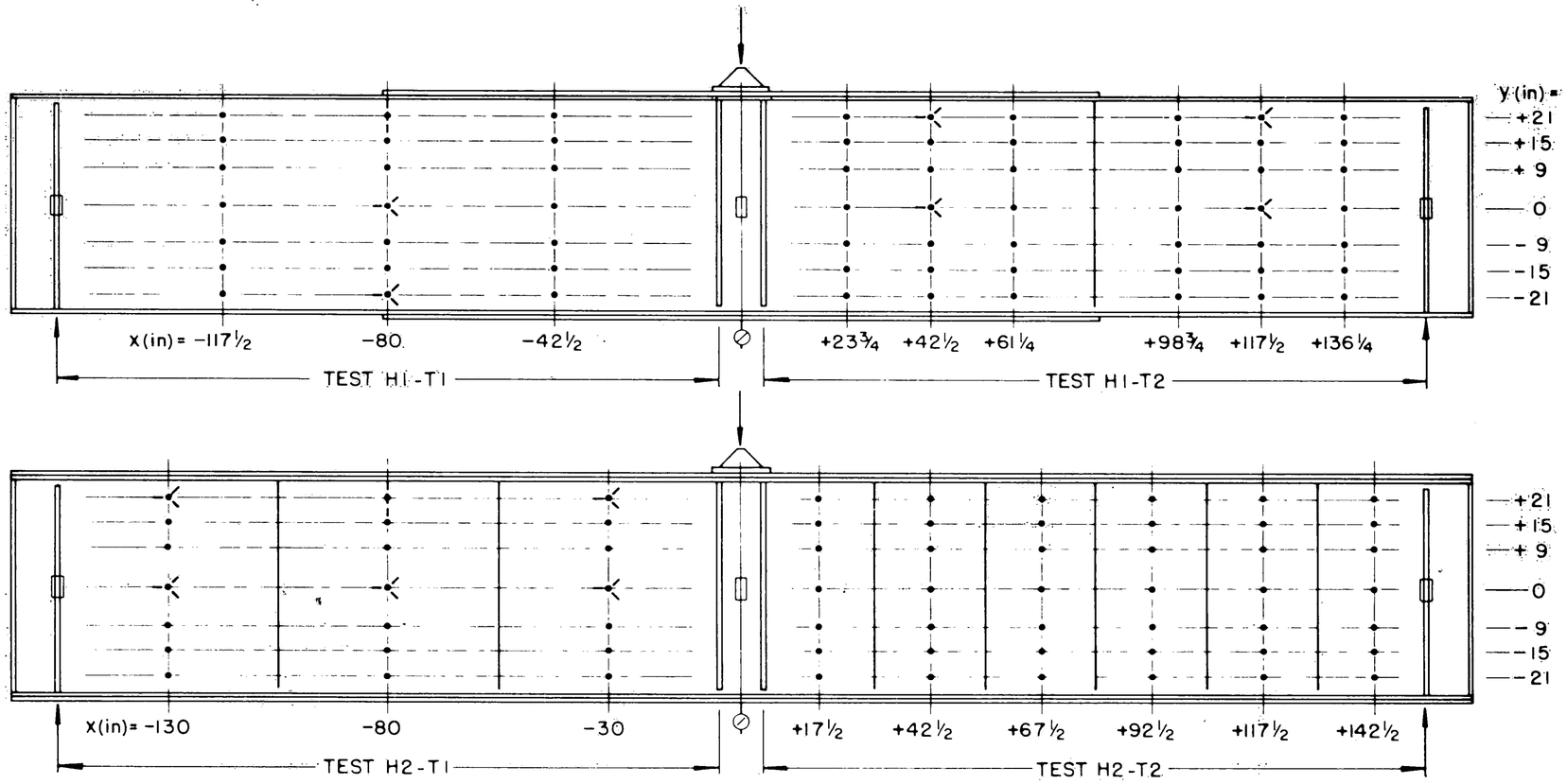

LEGEND

- Deflection scale
- location of web deflection measurements
- SR-4 gage rosettes
- Dial gage

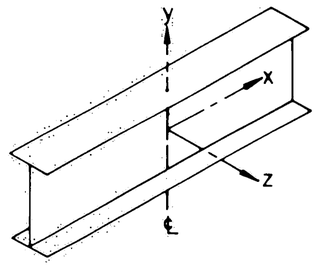

Fig. 8 Instrumentation

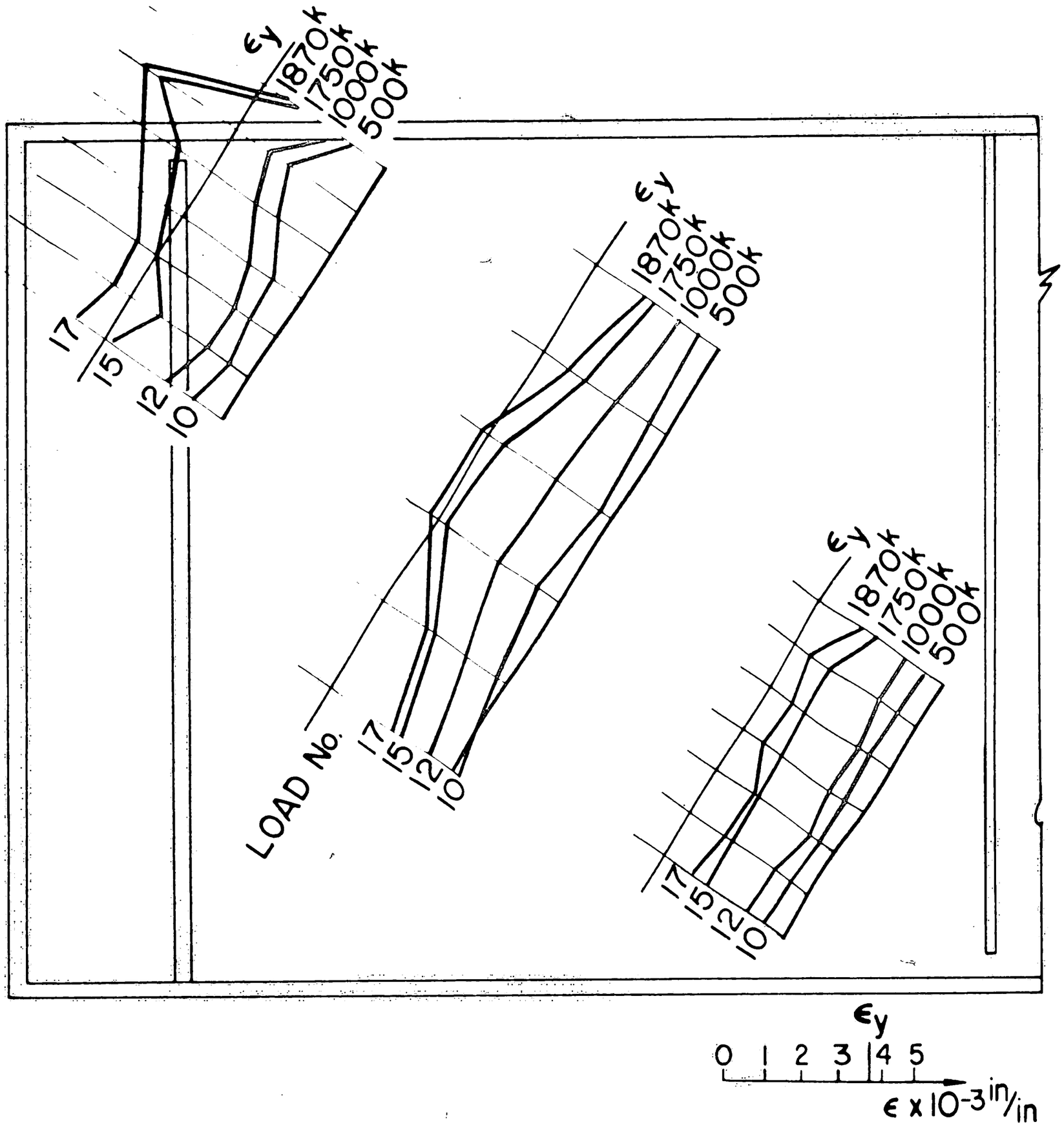

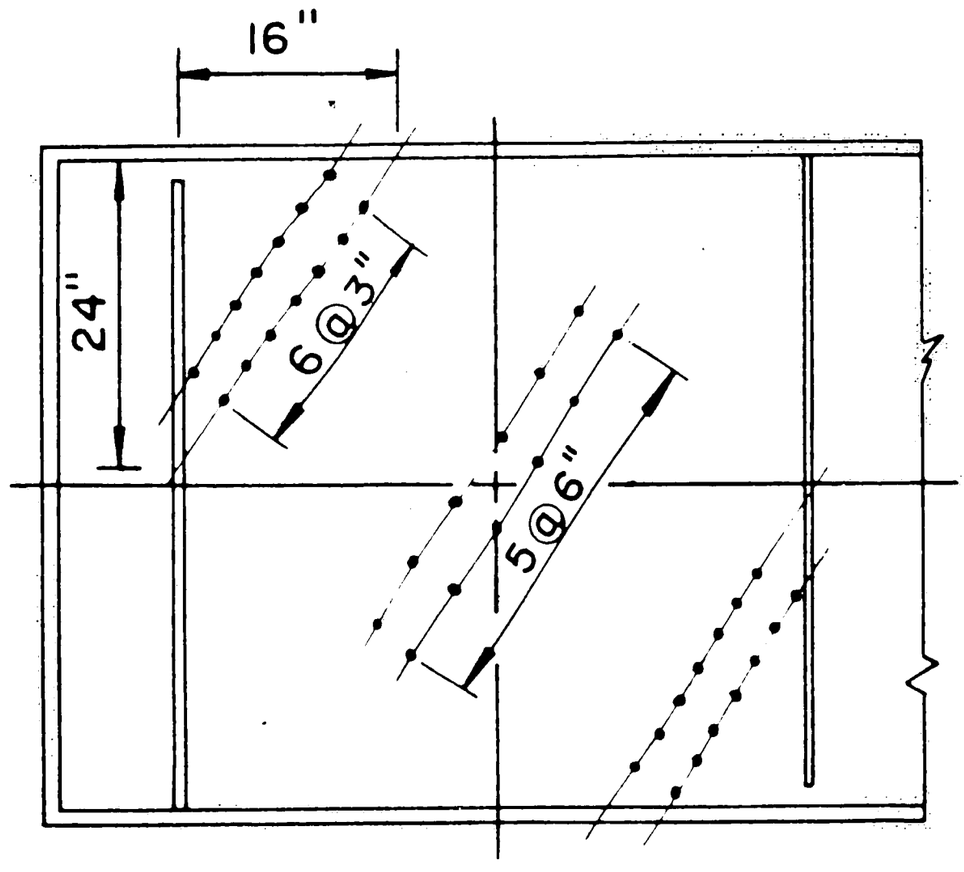

Fig. 9 Hand Extensometer Measurements, Test H2-T1

H1-T1

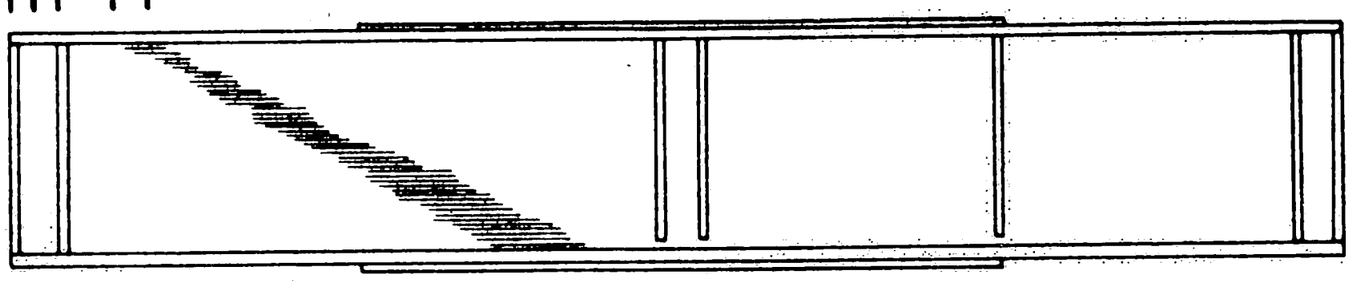

H1-T2

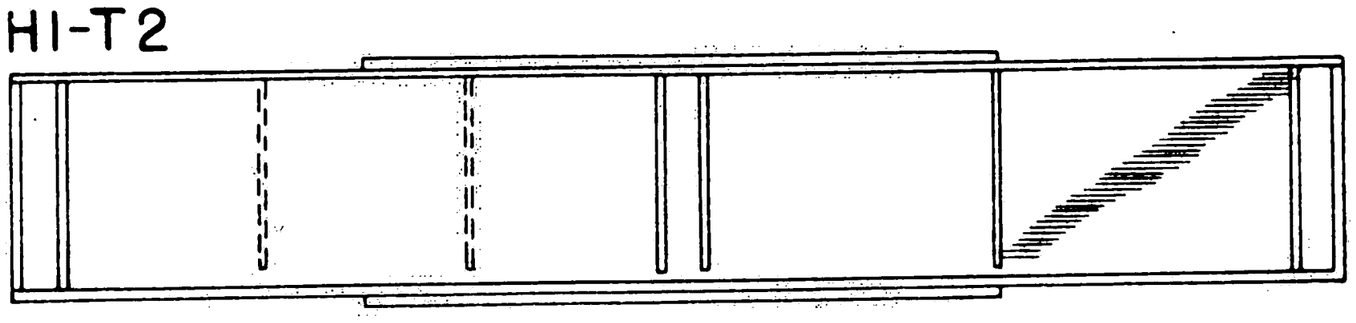

H2-T1

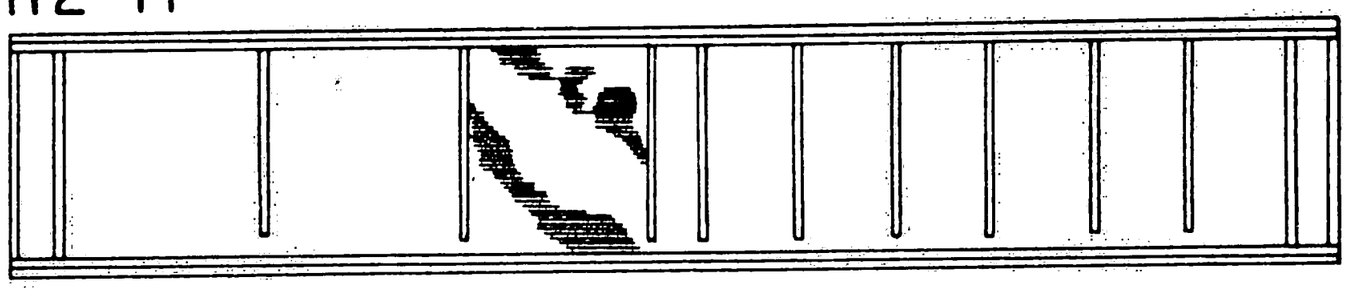

H2-T2

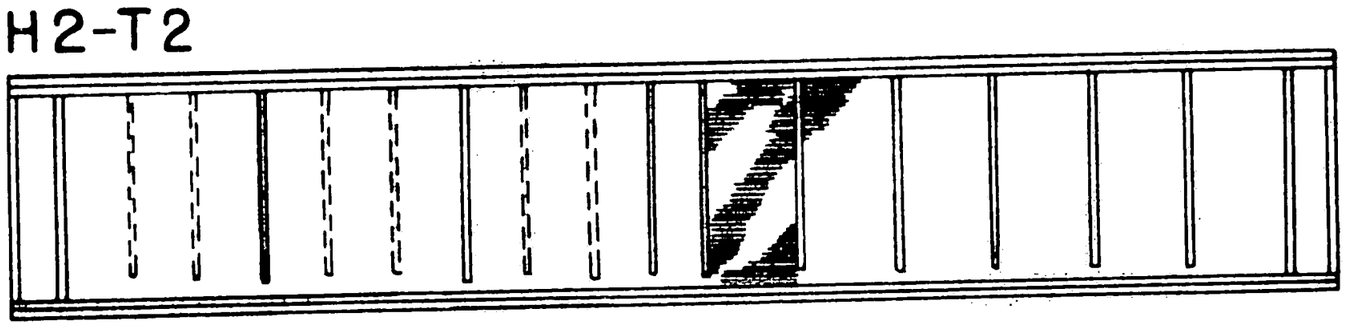

Fig. 10 Location of Girder Failures and Repairs

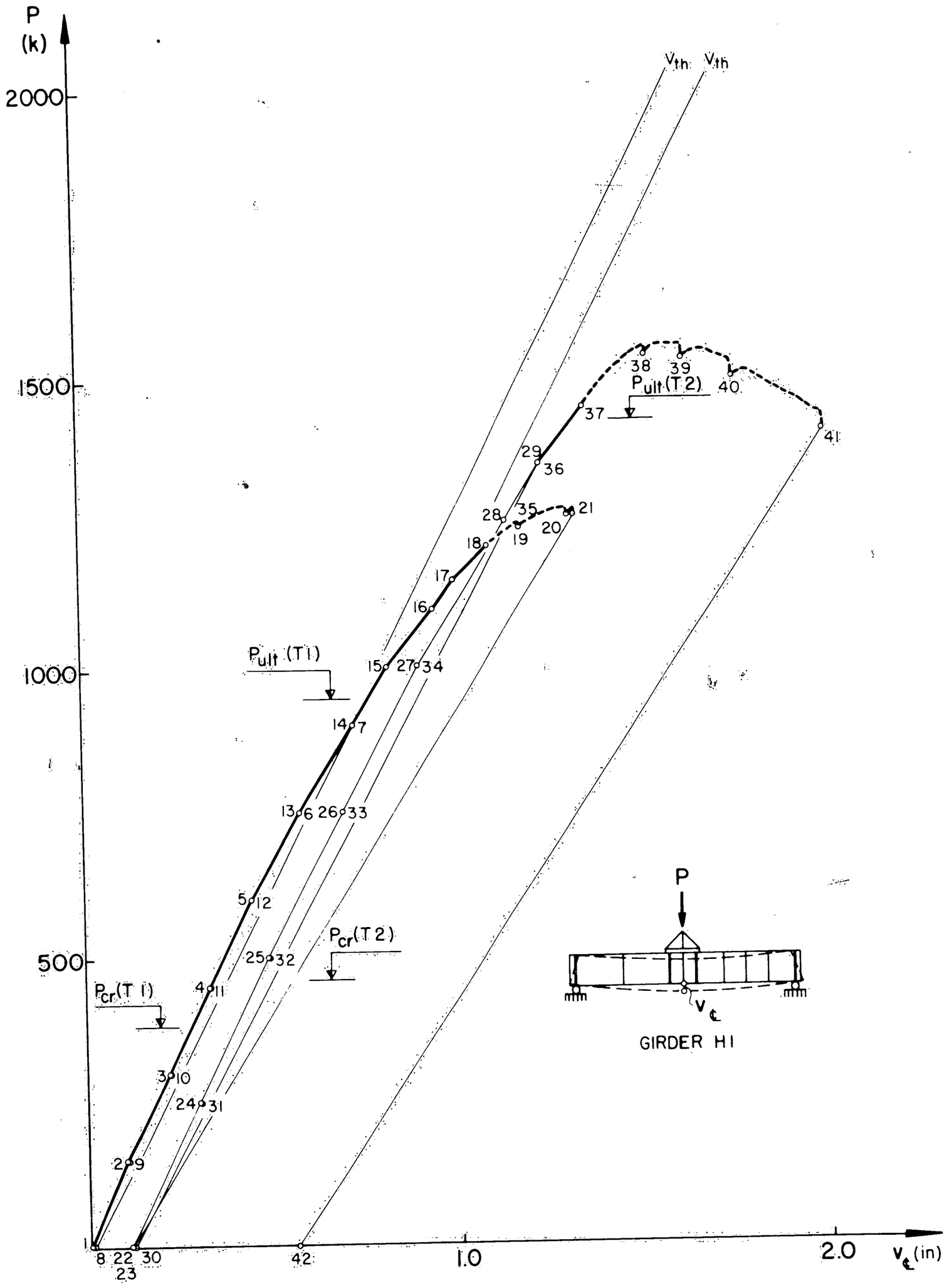

Fig. 11 Load-Deflection Diagram for Girder H1

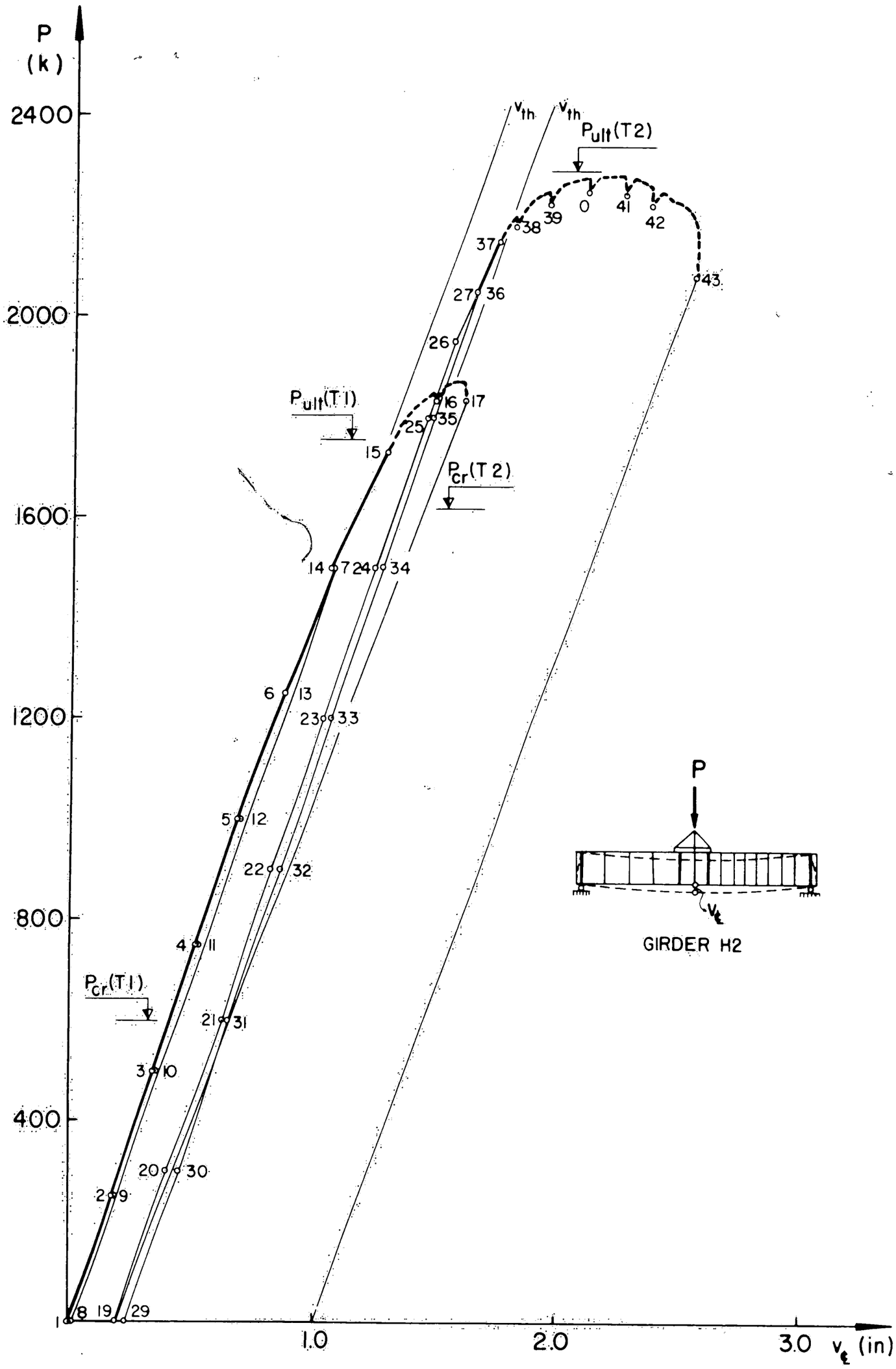

Fig. 12 Load-Deflection Diagram for Girder H2

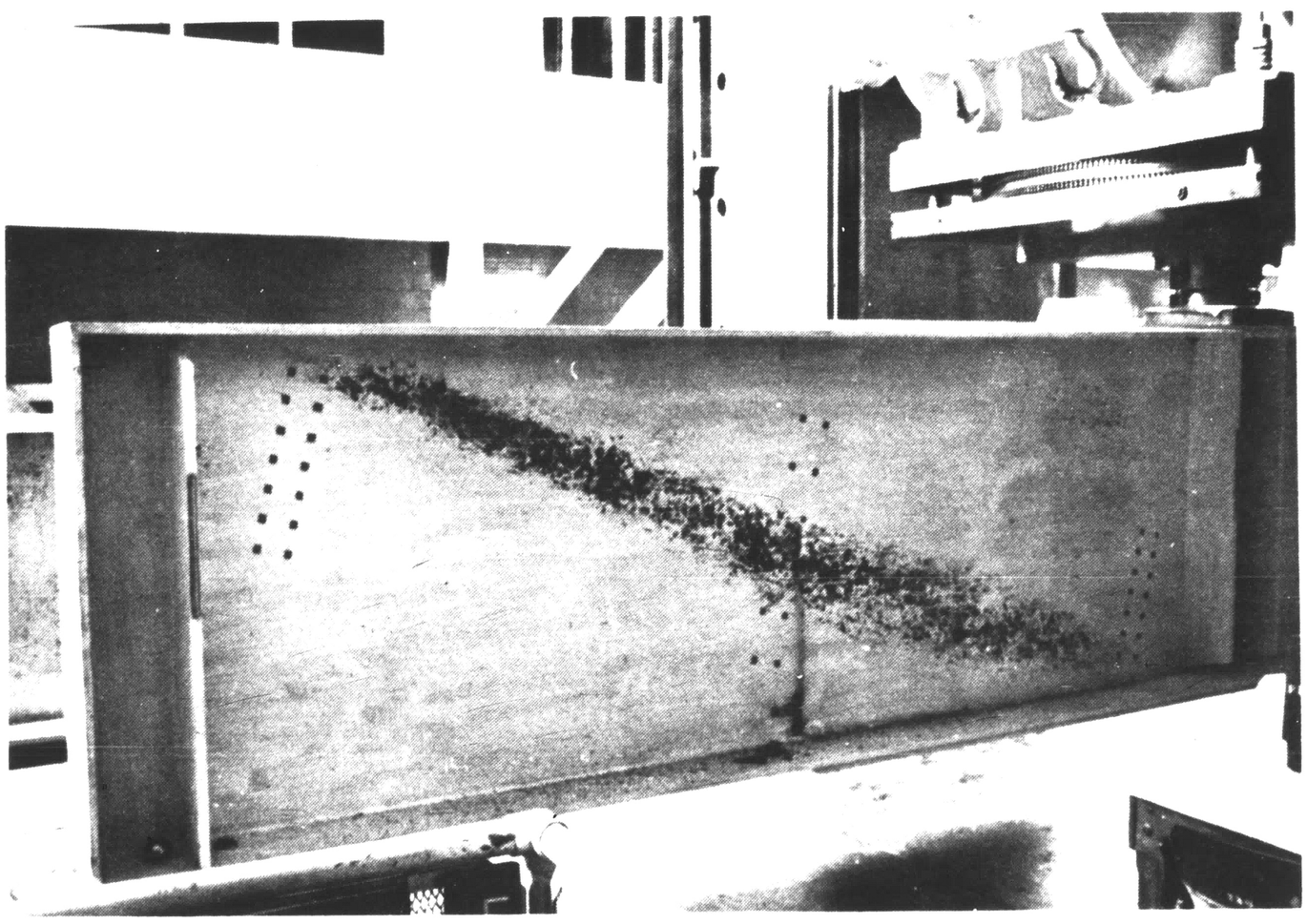

Fig. 13 Girder Panel at Failure, Test H1-T1

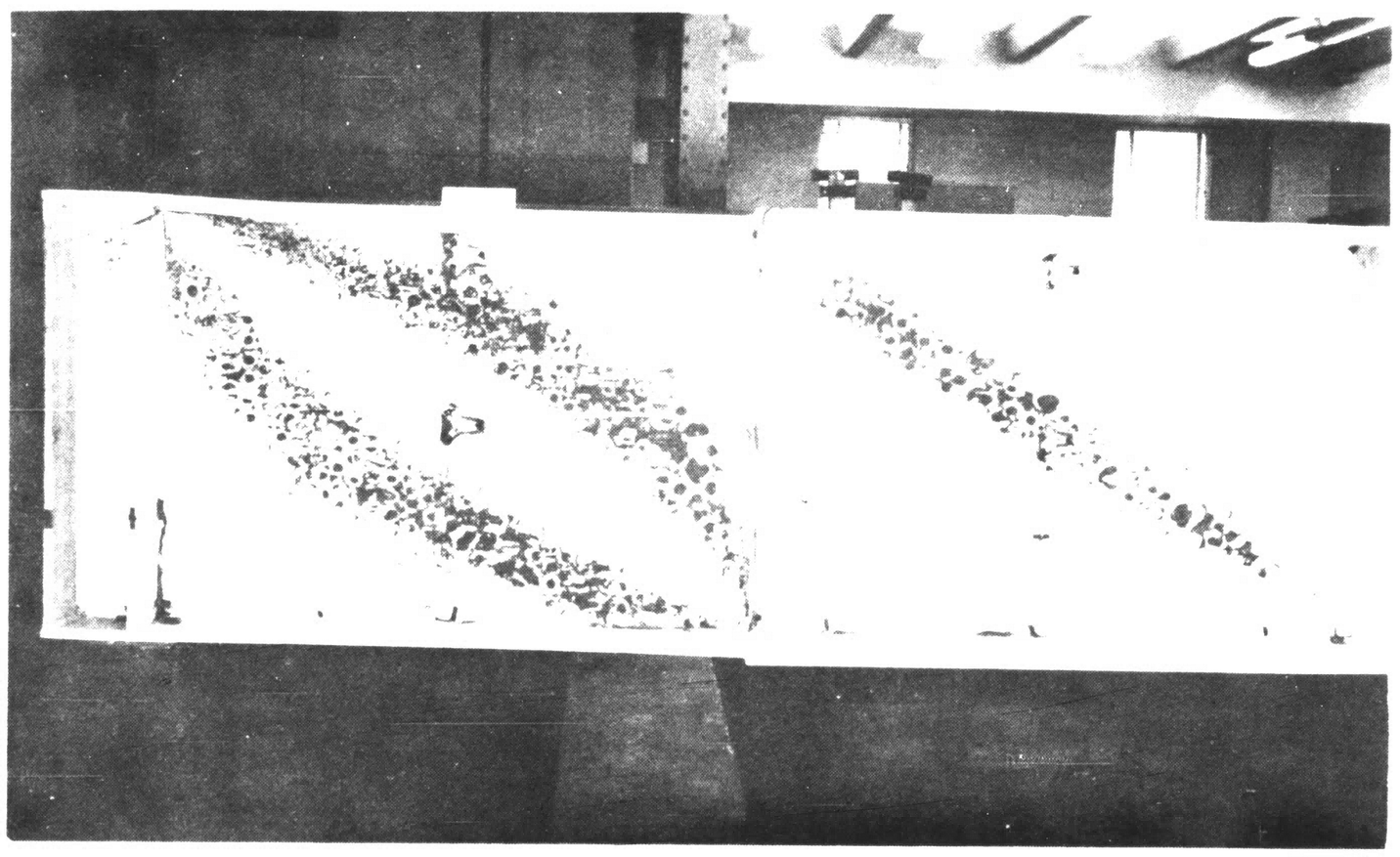

Fig. 14 Girder Appearance After Test H1-T2

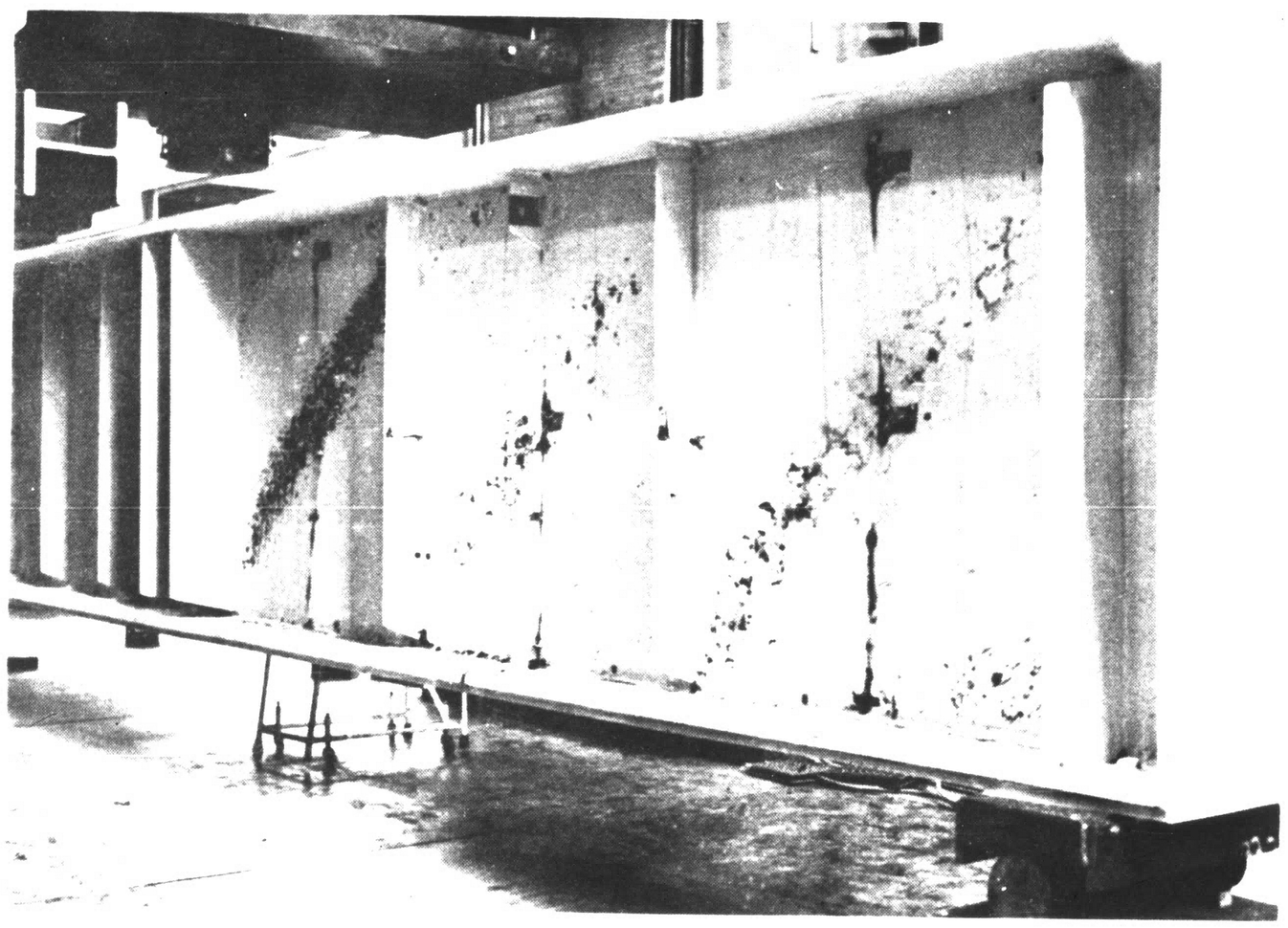

Fig. 15 Girder H2 After Test T1

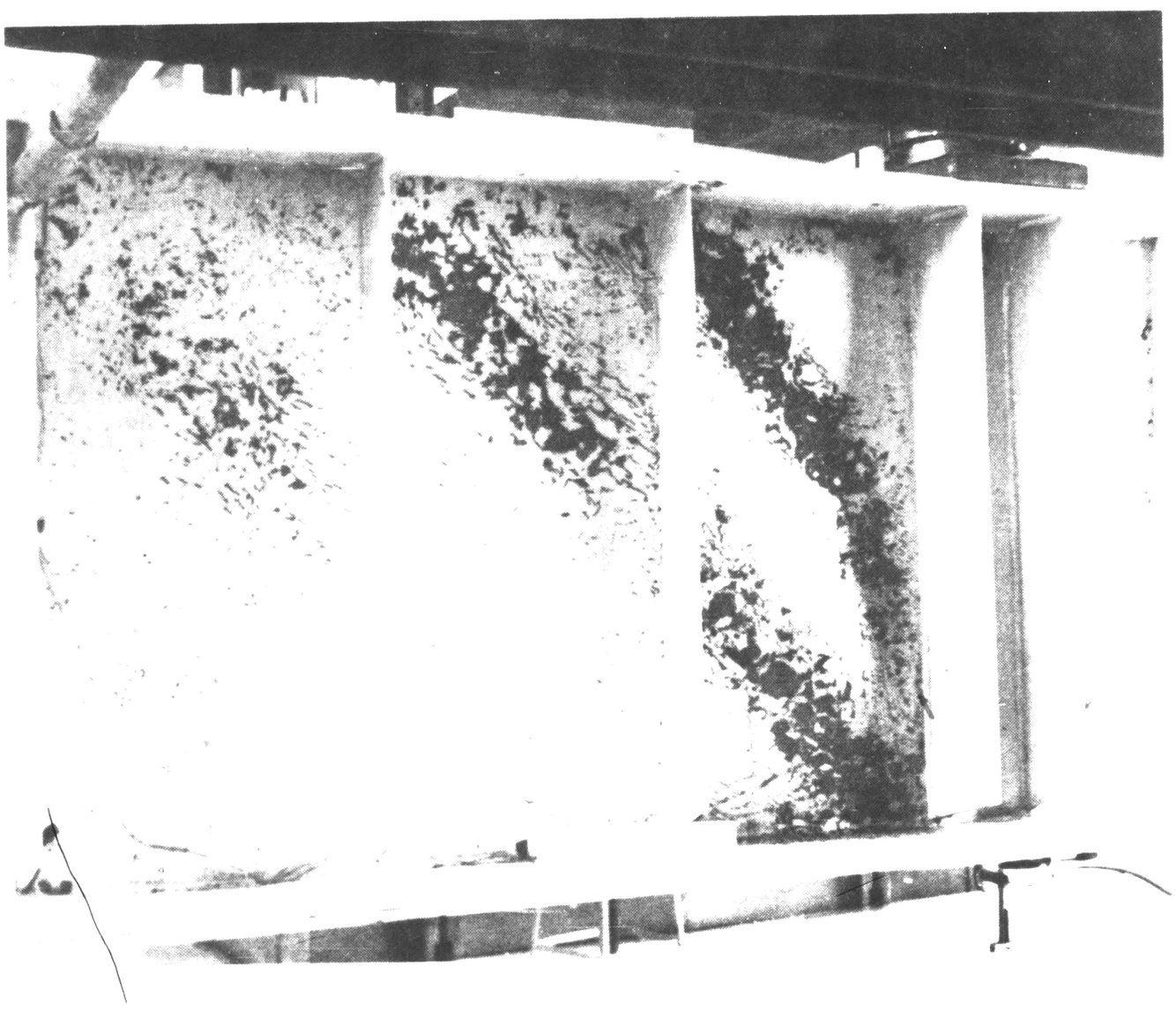

Fig. 16 Closeup After Ultimate Load, Test H2-T2

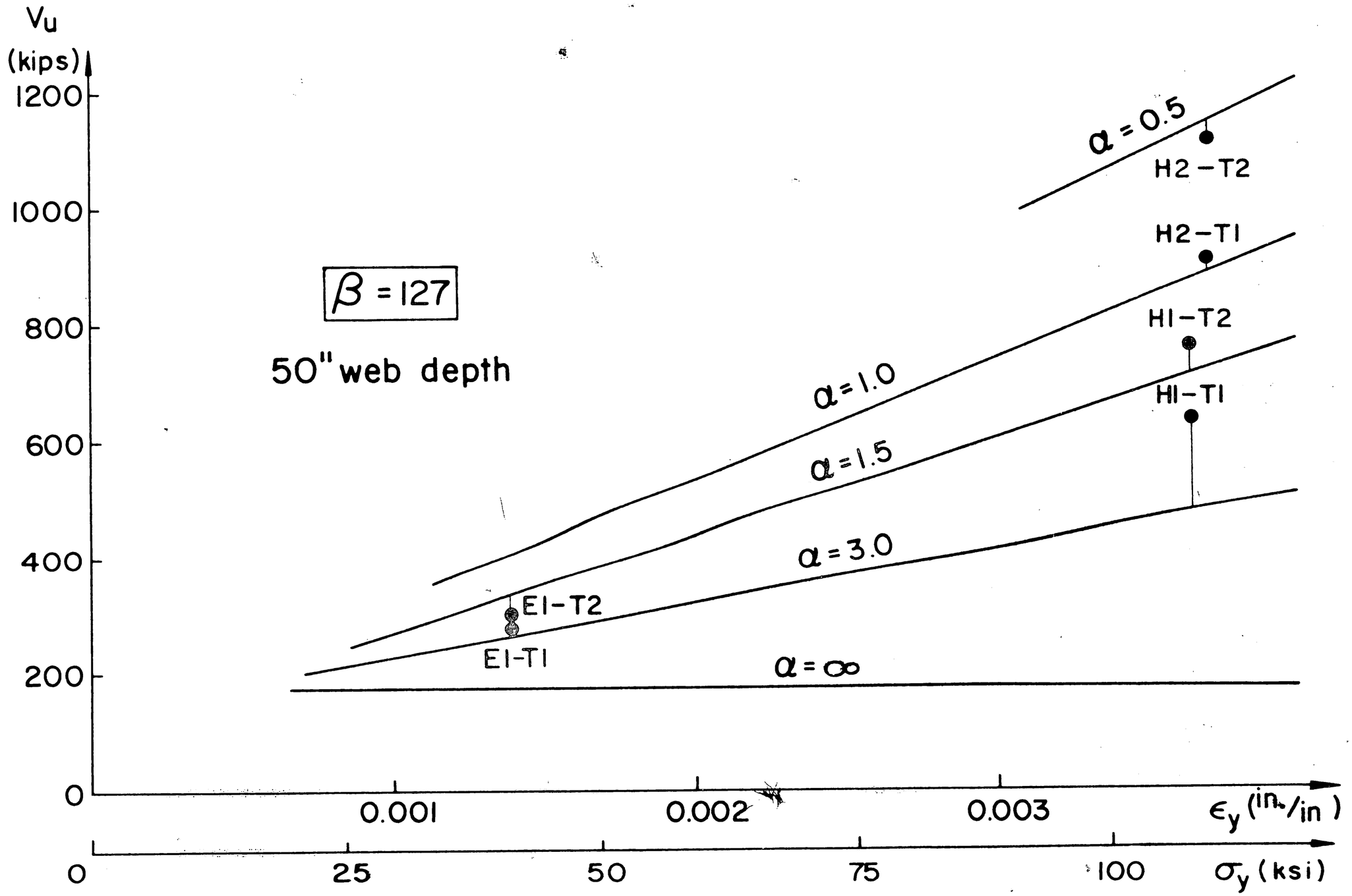

Fig. 17 Shear Strength vs. Yield Stress Diagram

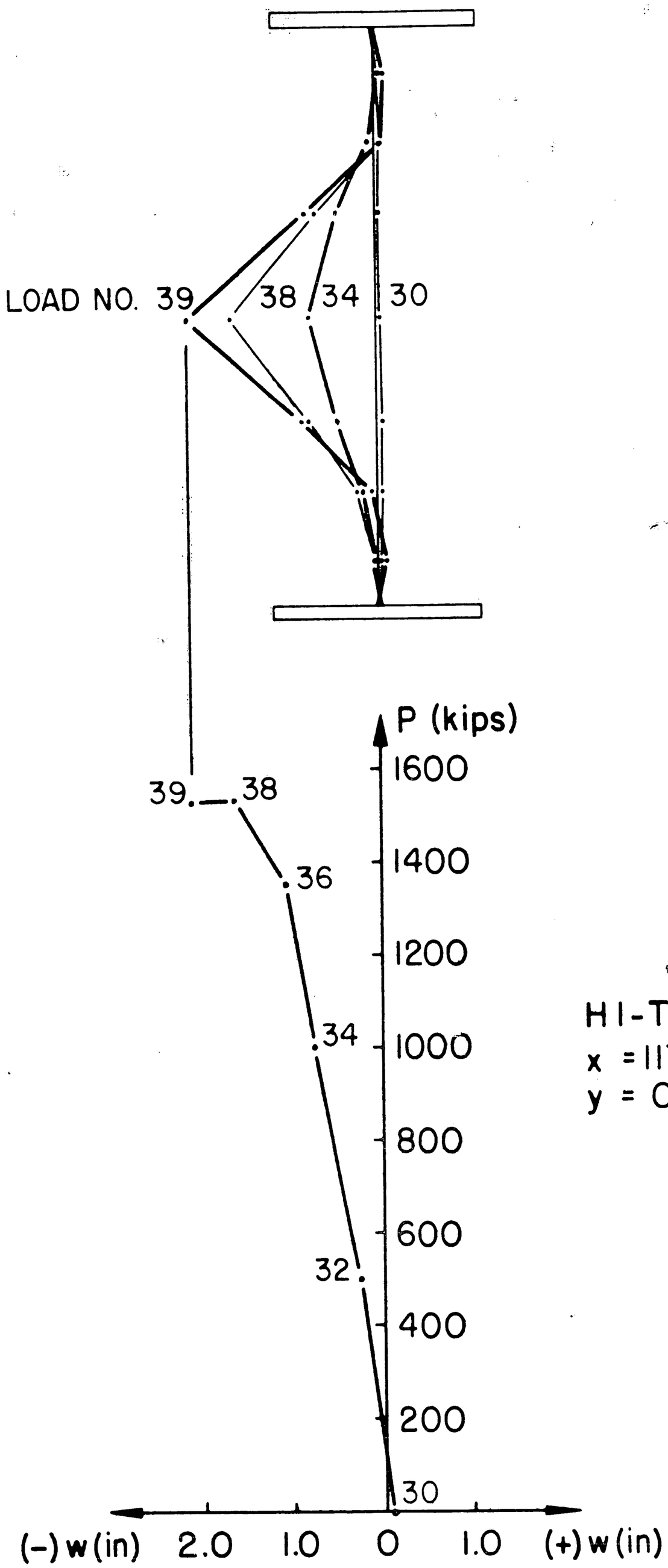

Fig. 18 Sample Web Deflection Curves

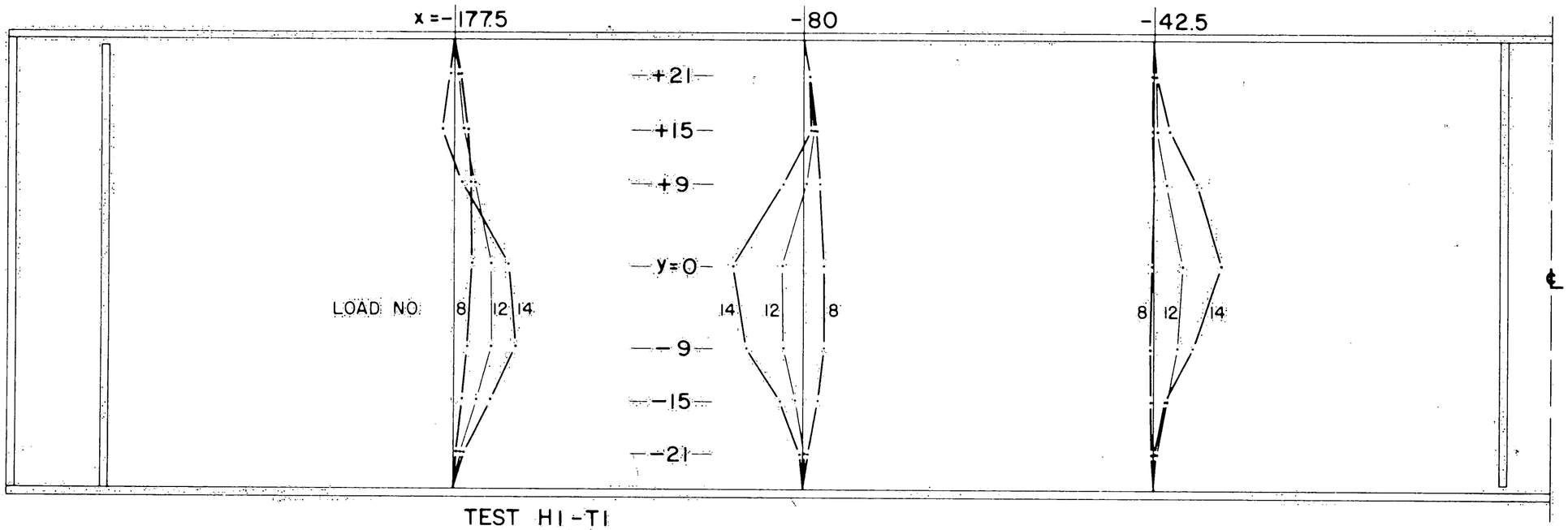

TEST H1-T1

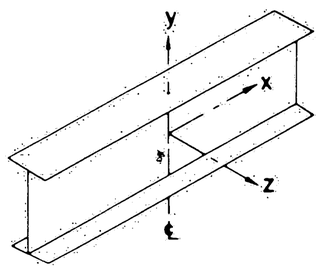

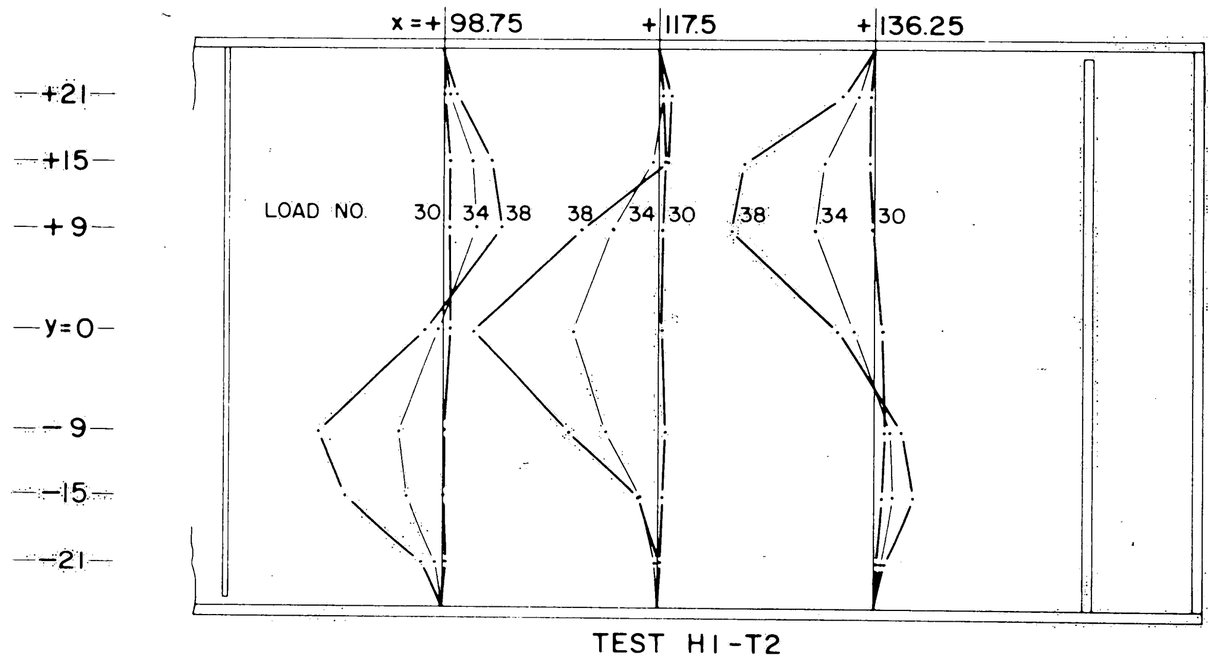

TEST H1-T2

Fig. 19 Web Deflections, Girder H1

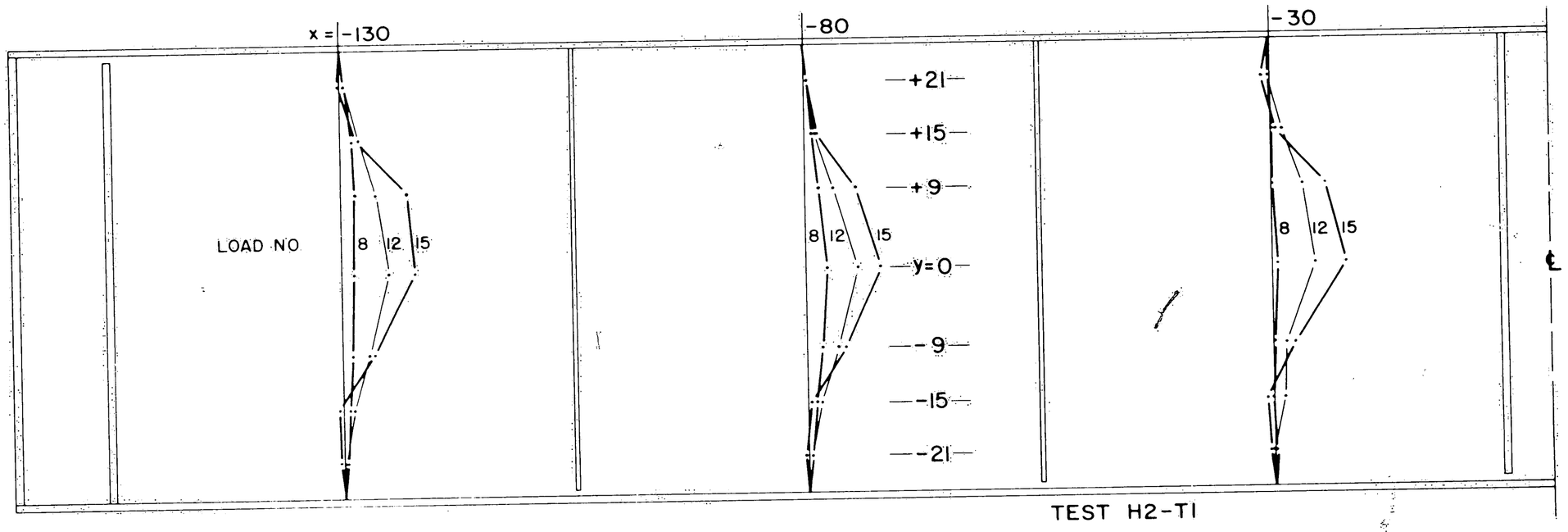

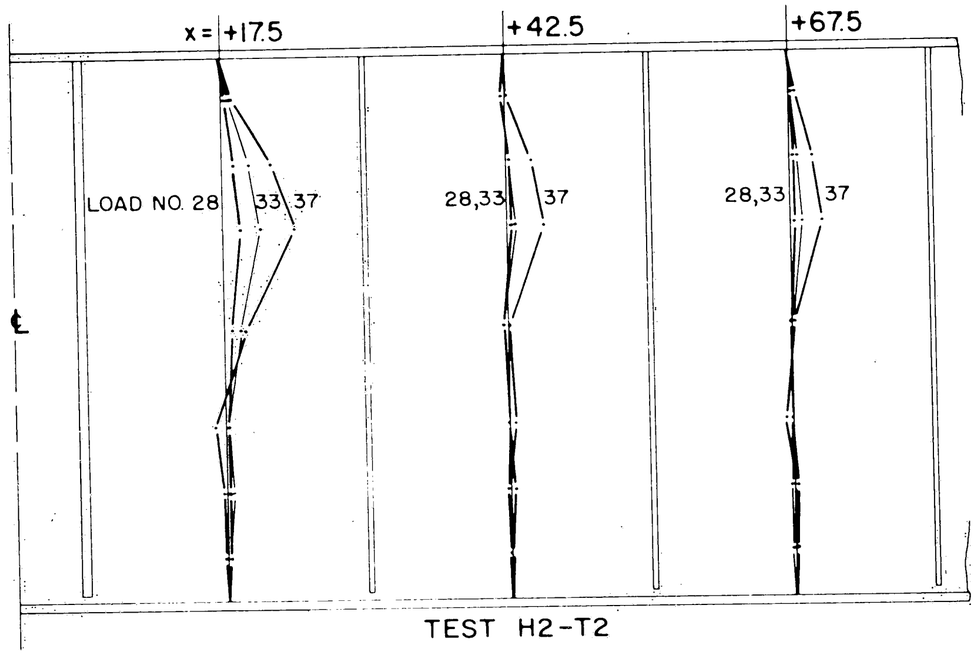

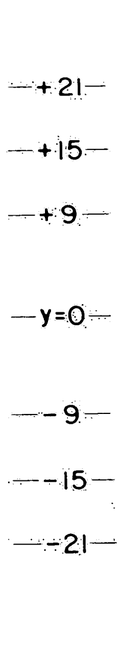

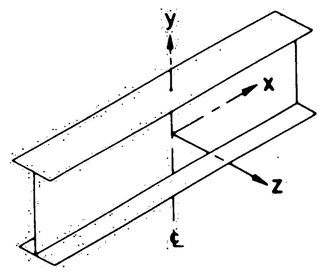

SCALE FOR w

0 ½ 1 in

Fig. 20 Web Deflections, Girder H2

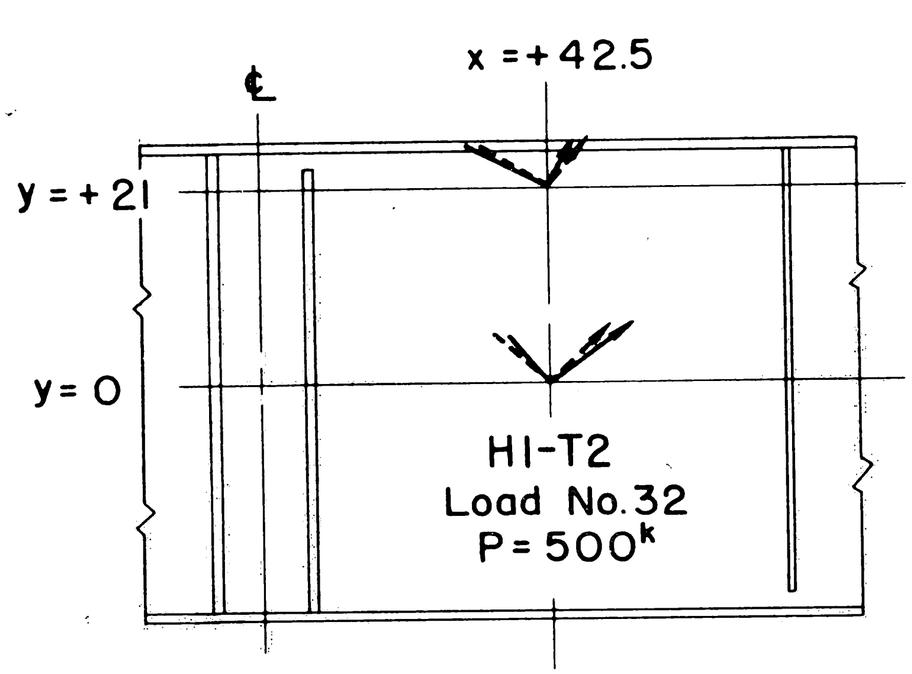

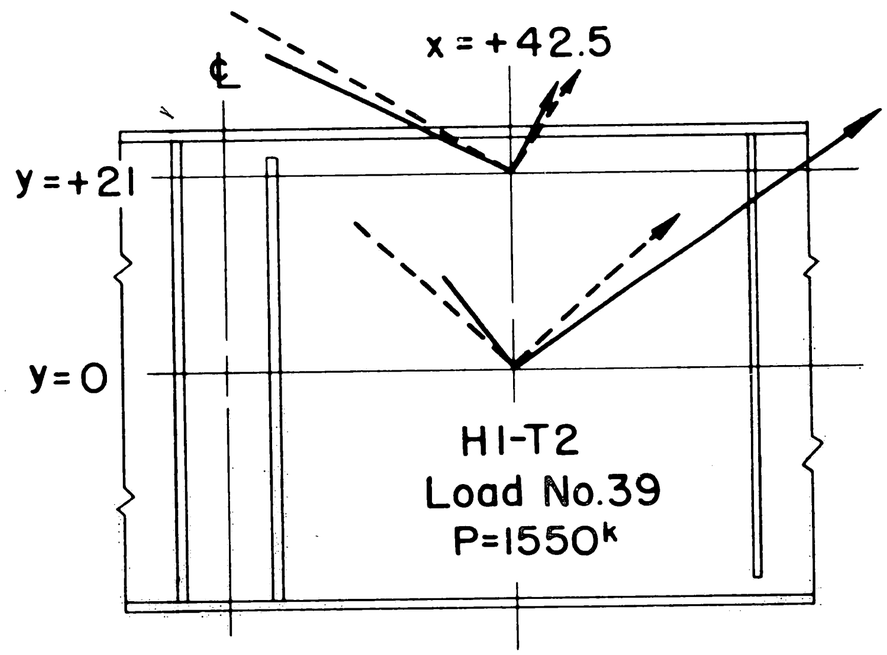

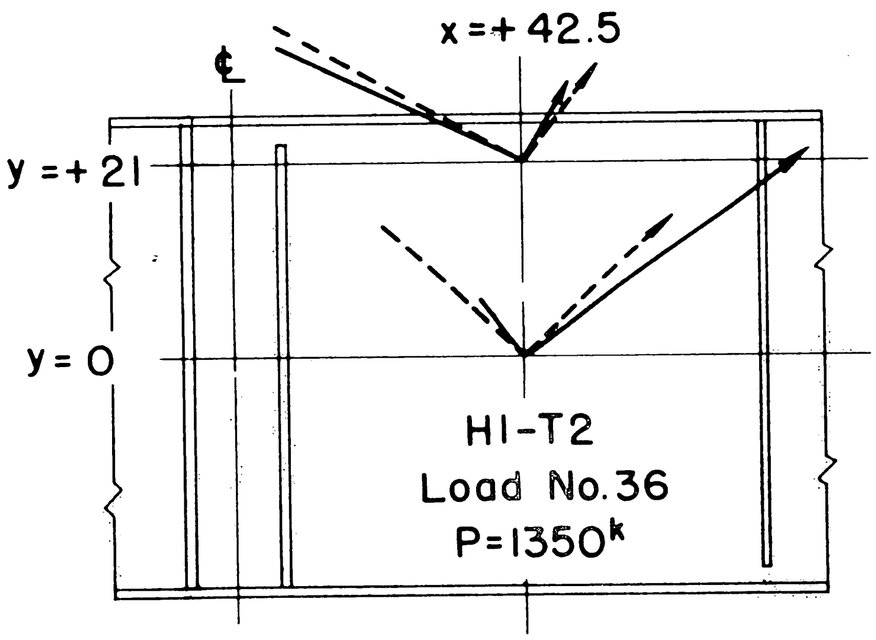

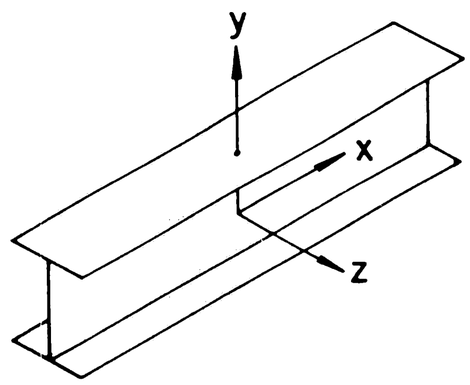

Scale for Stress 0 10 20 30 ksi

Compression Tension

——— Computed

——— Measured

Fig. 21 Principal Stresses in Web of Girder H1

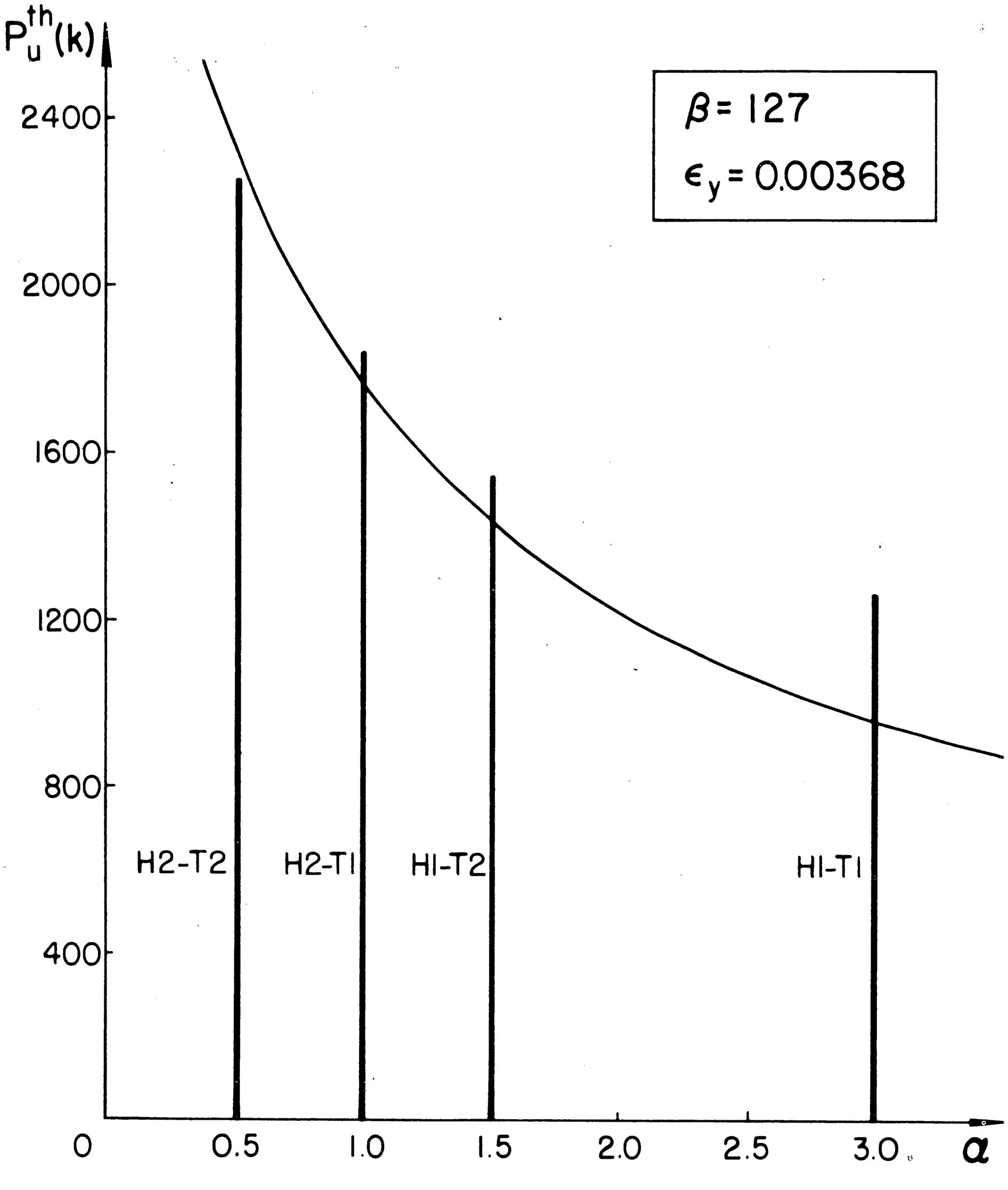

Fig. 22 Ultimate Load vs. Aspect Ratio Diagram

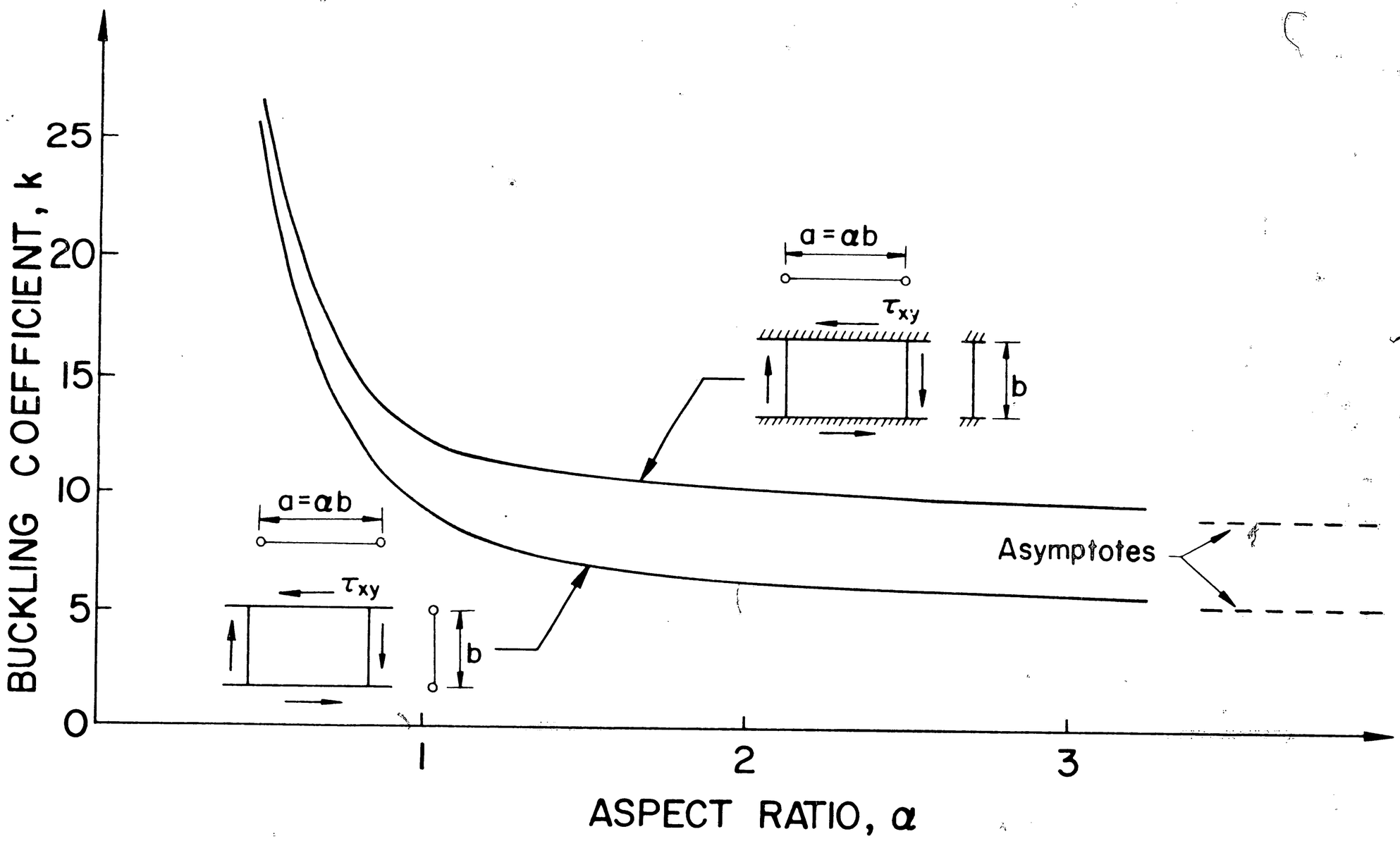

Fig. 23 Variation of Buckling Coefficient with Aspect Ratio

REFERENCES

1. Basler, K.
STRENGTH OF PLATE GIRDERS IN SHEAR
Proceedings, ASCE, Vol. 87, No. ST7, October, 1961

2. Basler, K., Yen, B. T., Mueller, J. A., and Thurlimann, B.
WEB BUCKLING TESTS ON WELDED PLATE GIRDERS
Bulletin No. 64, Welding Research Council
New York, September, 1960

3. Basler, K. and Thurlimann, B.
PLATE GIRDER RESEARCH
Proceedings, AISC Nat. Engrg. Conf., 1959

4. Basler, K.
STRENGTH OF PLATE GIRDERS UNDER COMBINED BENDING AND SHEAR
Proceedings, ASCE, Vol. 87, No. ST7, October, 1961

5. Basler, K.
FURTHER TESTS ON WELDED PLATE GIRDERS
Proceedings, AISC Nat. Engrg. Conf., 1960

6. Kollbrunner, C. F. and Meister, M.
AUSBEULEN
Springer-Verlag, Berlin, Gottingen and Heidelberg, 1958

7. Tall, Lambert
RESIDUAL STRESSES IN WELDED PLATES-A THEORETICAL STUDY
Fritz Laboratory Report No. 249.11, Lehigh University, Bethlehem, Pennsylvania, July, 1961

8. Basler, K. and Thurlimann, B.
STRENGTH OF PLATE GIRDERS IN BENDING
Proceedings, ASCE, Vol. 87, No. ST6, August, 1961

VITA

The author was born in Seoul, Korea on December 23, 1936, the fifth child of Sikook and Kyungsoo Lew.

He graduated from Yong San High School in Seoul, Korea in March, 1954 and then attended Washington University, St. Louis, Missouri from January, 1956 to June, 1960. There he completed the requirements of the Department of Architectural Engineering and was awarded the degree of Bachelor of Science.

In June, 1959 he joined the Bank Building and Equipment Corporation of America, and was employed as a structural engineer until September, 1961.

The author enrolled in the Graduate School, Department of Civil Engineering at Lehigh University, in September, 1961, and was appointed to a graduate assistantship in February, 1961 and later to a research assistant-ship in June, 1962 He has been associated with the Welded Plate Girder Project in the Structural Metals Division of Fritz Engineering Laboratory, Lehigh University since June, 1962.